

Detection of symmetry-protected topological phases in fermionic many-body systems

Hassan Shapourian, Ken Shiozaki, and Shinsei Ryu

Department of Physics, University of Illinois at Urbana-Champaign, Urbana Illinois 61801, USA

(Dated: October 11, 2024)

We present an approach to define and compute topological invariants of interacting fermionic symmetry-protected topological (SPT) phases, protected by an orientation-reversing symmetry, such as time-reversal or reflection symmetry. The topological invariants are given by partition functions on unoriented spacetime which as we show, can be computed for a given ground state wave function by considering a non-local operation, “partial” reflection or transpose. As an application of our scheme, we study the \mathbb{Z}_8 and \mathbb{Z}_{16} classification of topological superconductors in one and three dimensions.

The discovery of topological insulators and superconductors [1, 2] has led to a new research frontier in condensed matter physics, generally referred to as symmetry protected topological (SPT) phases. A complete classification of the noninteracting fermionic SPT phases in the presence of non-spatial discrete symmetries was achieved [3–5]. The noninteracting classification was further generalized to encompass crystalline SPT phases with spatial symmetries, such as reflection [6–9]. The classification of interacting fermions was pioneered in Refs. [10, 11], where it was found that the noninteracting classification can be dramatically changed when interactions are taken into account. Since then, there have been several works which discuss the breakdown or collapse of the non-interacting classification of fermionic SPT phases in the presence of interactions [12–23].

It has been recently claimed that the cobordism theory can provide a complete classification of both fermionic and bosonic interacting SPT phases in all dimensions [24–28], which goes beyond the group cohomology classification [29, 30]. In particular, for SPT phases protected by orientation-reversing symmetry, it has been found that the partition function of topological quantum field theories defined on unoriented spacetimes can be used to identify interacting SPT phases [22, 24, 25, 27, 31–34].

In this letter, we translate this mathematical description (cobordism theory) to a practical procedure; we propose methods of extracting many-body topological invariants (SPT invariants) for a given microscopic model. We provide two different implementations. First, by using the spacetime path integral, we explain how one can simulate unoriented spacetime manifolds by introducing a cross-cap in the spacetime, which can be constructed by using time-reversal or reflection. Second, for both symmetries, we introduce an SPT invariant that can be written in terms of a ground state wave function as an expectation value of a non-local operator (“partial transformation”). In particular, we provide explicit calculations for one dimensional models in the symmetry classes BDI (protected by time-reversal symmetry), D and A with reflection symmetry. We also briefly discuss higher dimensional extensions of this idea and calculate the many-body SPT invariant for three-dimensional topological su-

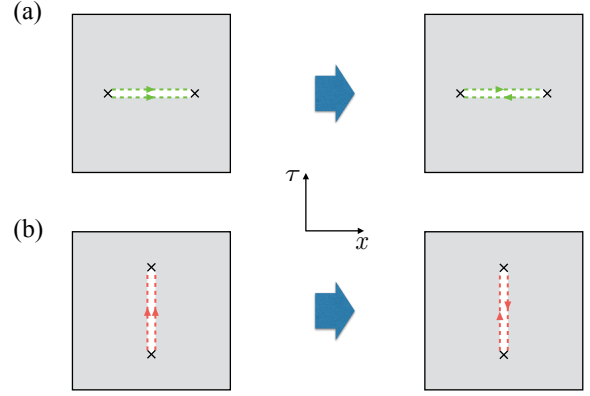


FIG. 1. Realization of a cross-cap in the spacetime. First and second columns show the original connectivity after cutting and the twisted bonding after gluing, respectively. (a) Spatial reflection, and (b) time inversion.

perconductors in symmetry class D with inversion symmetry.

We emphasize that the proposed SPT invariants are many-body topological invariants, which do not require a single-particle description. They thus have the same status as the topological invariants written in terms of response functions, such as the Hall conductance (the many-body Chern number).

One-dimensional topological superconductors in symmetry classes $D+R_-$ and BDI_- —We will describe our scheme by using examples of one-dimensional topological superconductors in class BDI (characterized by time-reversal symmetry where $\mathcal{T}^2 = 1$), or class D with reflection symmetry (characterized by reflection symmetry where $\mathcal{R}^2 = (-1)^F$ and F is the fermion number). The latter case is referred to as symmetry class “ $D+R_-$ ” in Refs. [7–9]. In addition to these symmetries, the fermion number parity $(-1)^F$ is also conserved in these systems. The topological superconductors in these symmetry classes are classified by an integer topological invariant at the free fermion level [7–9]. The integral classification of these noninteracting systems collapses into the \mathbb{Z}_8 classification in the presence of interactions [10, 35]. A canonical example of non-trivial topological supercon-

ductors in these symmetry class is given by the Kitaev Majorana chain Hamiltonian [36]

$$\hat{H} = - \sum_x \left[t f_{x+1}^\dagger f_x - \Delta f_{x+1}^\dagger f_x^\dagger + \text{H.c.} \right] - \mu \sum_x f_x^\dagger f_x, \quad (1)$$

which describes a superconducting state of spinless fermions. For simplicity, we set $t = \Delta$ in the following. (Δ is taken as a real parameter unless otherwise stated.) The SPT phase in this model, realized when $|\mu|/t < 2$, is protected either by reflection $\mathcal{R}f_x\mathcal{R}^{-1} = if_{-x}$, or time-reversal $\mathcal{T}f_x\mathcal{T}^{-1} = f_x$, $\mathcal{T}i\mathcal{T}^{-1} = -i$.

As shown in Ref. [27], effective actions of fermionic topological SPT phases protected by an orientation-reversing symmetry (either time-reversal symmetry $\mathcal{T}^2 = 1$, or reflection symmetry $\mathcal{R}^2 = (-1)^F$) in d dimensional spacetime are classified by elements of the cobordism group $\text{Hom}(\Omega_d^{Pin^-}, U(1))$, where $\Omega_d^{Pin^-}$ is the group of bordism classes of manifolds of dimension d with Pin^- structure. In particular, for $d = 1+1$ dimensional models the bordism group is $\Omega_2^{Pin^-} = \mathbb{Z}_8$ and generated by the real projective plane $\mathbb{R}P^2$. This means that the partition function of the generating model (which is the Majorana chain (1) in this case) on $\mathbb{R}P^2$ would give a $\mathbb{Z}_8 \in U(1)$ phase (the eighth root of unity).

Spacetime path-integral.— As clear from the above discussion, the complex phase of partition function, when the system is put on an appropriate (unoriented) spacetime manifold, serves as an SPT invariant [37]. We start from the ordinary Euclidean path integral representation of the partition function

$$Z = \text{Tr}(e^{-\beta\hat{H}}) = \int \mathcal{D}[\xi]\mathcal{D}[\bar{\xi}] e^{-S[\bar{\xi},\xi]}, \quad (2)$$

where $S[\bar{\xi},\xi] = \int_0^\beta d\tau [\bar{\xi}\partial_\tau\xi + H(\bar{\xi},\xi)]$, and τ is the continuous time, and the Grassmann variables $\xi(\tau,x)$ and $\bar{\xi}(\tau,x)$ are defined at time τ and real-space position x , and obey the anti-periodic temporal boundary condition, $\xi(\tau+\beta) = -\xi(\tau)$, $\bar{\xi}(\tau+\beta) = -\bar{\xi}(\tau)$.

In the path integral, one way to obtain $\mathbb{R}P^2$ as the spacetime manifold is to introduce a cross-cap (Fig. 1). The procedure is to make a cut in the spacetime and glue back. Depending on the type of orientation-reversing symmetry in question (i.e., reflection or time-reversal), the cut must be along the space direction (Fig. 1(a)) or along the time direction (Fig. 1(b)), respectively.

Next, the cut has to be glued back by using the orientation-reversing symmetry. For symmetry class $D+R_-$, we introduce the cross-cap by modifying the temporal boundary condition at $\tau = \beta \equiv 0$ as

$$\begin{aligned} \xi(\beta + \epsilon, x) &= -\xi(0, x) \rightarrow -i\xi(0, -x), \\ \bar{\xi}(\beta + \epsilon, x) &= -\bar{\xi}(0, x) \rightarrow i\bar{\xi}(0, -x), \end{aligned} \quad (3)$$

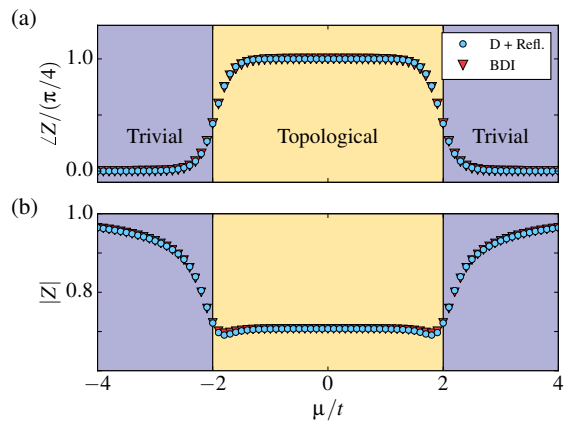


FIG. 2. Amplitude and phase of the partition function in the presence of spatial and temporal cross-caps (Details in Appendix A).

over a lattice segment $x_1 < x < x_2$ where the reflection is done with respect to a vertical line crossing the central bond of the segment (see Fig. 1(a)). Here, ϵ is the discretization step along the time axis, $\epsilon = \beta/N_t$.

As for symmetry class BDI, we first note that in the path-integral formalism the time-reversal symmetry, which is an antiunitary transformation in the operator formalism, should be implemented as an invariance of the path-integral under a change of path-integral variables. In the case of fermions, time-reversal transformation is equivalent to the change of Grassmann fields as in

$$\xi(\tau, x) \rightarrow i\bar{\xi}(\beta - \tau, x), \quad \bar{\xi}(\tau, x) \rightarrow i\xi(\beta - \tau, x). \quad (4)$$

One can check that the transformation (4) leaves the Hamiltonian (1) or, in fact, more generic bilinear forms $H(\bar{\xi}, \xi) = \sum_{x,x'} [t_{xx'}\bar{\xi}(x)\xi(x') + \Delta_{xx'}\bar{\xi}(x)\bar{\xi}(x') + \text{H.c.}]$ invariant. It is easy to see that possible two-body interaction terms such as $(\bar{\xi}\xi)^2$ are also invariant. A time-reversal cross-cap can then be implemented by twisting the spatial boundary condition into

$$\begin{aligned} \xi(\tau, N+1) &= -\xi(\tau, 0) \rightarrow -i\bar{\xi}(\tilde{\tau}, 0), \\ \bar{\xi}(\tau, N+1) &= -\bar{\xi}(\tau, 0) \rightarrow -i\xi(\tilde{\tau}, 0), \end{aligned} \quad (5)$$

over a time interval $t_1 < \tau < t_2$ where $0 < t_1, t_2 < \beta$ and the time inversion $\tau \rightarrow \tilde{\tau}$ is performed with respect to the central line $\tau = (t_1 + t_2)/2$ of the interval (see Fig. 1(b)).

The numerically computed partition function in the presence of a cross-cap is shown in Fig. 2. The results for the symmetry classes BDI and $D+R_-$ match with each other. Well inside the SPT phase (realized for $|\mu|/t < 2$), the partition function is given by

$$Z \sim e^{i\frac{\pi}{4}}/\sqrt{2}, \quad (6)$$

whereas in the trivial phase $Z \leq 1$ with no complex phase; Z approaches one as one goes deep inside the triv-

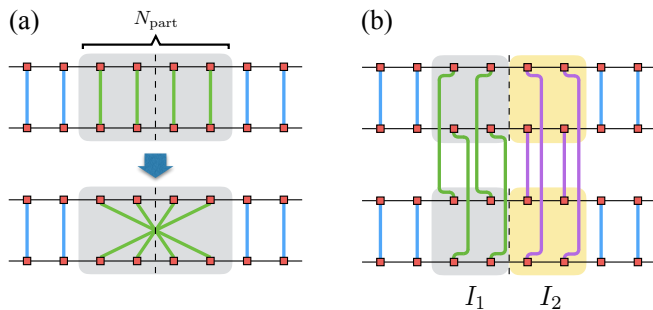


FIG. 3. Schematic representation of a cross-cap for the ground state overlap (a) partial reflection, $\langle \Psi | \mathcal{R}_{\text{part}} | \Psi \rangle$, (b) partial transpose, $\text{tr}(\rho_I U_T^{I_1} \rho_I^{T_1} [U_T^{I_1}]^\dagger)$. Solid squares represent physical sites and vertical bonds represent how physical dof contracted between $|\Psi\rangle$ and $\langle \Psi|$. The horizontal bonds show auxiliary dof (spatial correlations).

ial phase. The phase factor $e^{i\frac{\pi}{4}}$ is the \mathbb{Z}_8 phase associated with the partition function on $\mathbb{R}P^2$ and is additive as the number of fermion flavors is increased. We shall explain more about the amplitude $|Z|$ in the following section.

Partial reflection.— The cross-cap in the path-integral can also be implemented solely in terms of ground state wave functions of the fermionic SPT phases. Let us now discuss this “operator formalism”.

First, the reflection cross-cap can be expressed as the expectation value of a non-local operator $\mathcal{R}_{\text{part}}$ for a given wave function (Fig. 3 (a)),

$$Z_{\mathcal{R}} = \langle \Psi | \mathcal{R}_{\text{part}} | \Psi \rangle \quad (7)$$

where $\mathcal{R}_{\text{part}}$ is the *partial reflection* operator which reflects the sites within a segment of lattice with respect to its central bond (dashed line in Fig. 3). This quantity has been first proposed as a non-local order parameter to distinguish various topological phases of spin chains [38–40]. As we show here, the overlap $Z_{\mathcal{R}}$ can also be used as an effective method to extract the SPT invariant in the reflection symmetric fermionic SPT phases.

Here, we examine the idea of partial reflection for SPT phases in symmetry class $D+R_-$ using the example of the Kitaev chain (1). Using the definition of reflection symmetry in this model, we can construct $\mathcal{R}_{\text{part}}$ and compute $Z_{\mathcal{R}}$. The result summarized in Fig. 4 confirms that (7) shows the similar behavior as its path-integral counterpart. (An analytical derivation of the same result for the fixed point wave function at $\mu = 0$ is provided in Appendix C). More examples including the *s*-wave superconducting nanowire construction [41] of Majorana chain, and the symmetry class A with reflection are provided in Appendix E.

Few remarks regarding the amplitude $|Z|$ are in order. First, in the topological phase, the factor $\sqrt{2}$ in the denominator is the quantum dimension of Majorana fermions and physically related to breaking two bonds

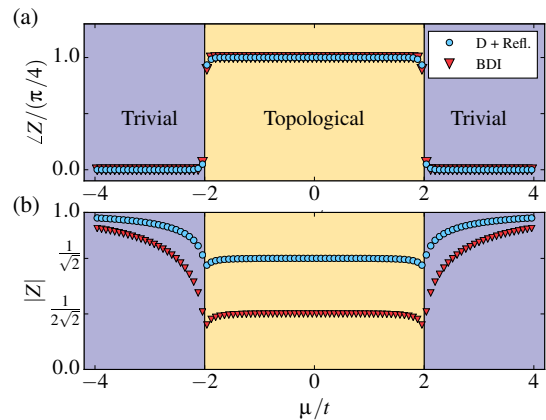


FIG. 4. Partial reflection (Eq. (7)) for class D with reflection and partial transpose (Eq. (9)) for class BDI in the Kitaev Majorana chain. Here, $N = 120$ and $N_{\text{part}} = 60$. For partial transpose, I_1 and I_2 each has 30 sites.

between the adjacent fermion sites. For instance, in the case of class A, $|Z| = 1/2$ in the topological phase corresponding to the quantum dimension of fermionic bound states (as opposed to Majoranas) at the ends. Second, in the trivial phase $|Z|$ is 1 only in the infinite gap limit and the smooth transition from $1/\sqrt{2}$ to 1 indicates finite size effects. Another important fact is that Z is a bulk quantity and hence independent of the physical boundary conditions at the ends of the chain (in the thermodynamic limit or long chain). Moreover, Z does not depend on the fermion parity of the wave function as well as the phase ϕ associated with the pairing potential $\Delta = |\Delta|e^{i\phi}$.

Partial transpose for bosons.— Let us now discuss the way to implement the time-reversal cross-cap in terms of a given ground state wave function. We first explain this briefly for one dimensional bosonic SPT phases with time-reversal symmetry $\mathcal{T} = U_T \mathcal{K}$ where \mathcal{K} is the complex conjugation and U_T is a unitary acting on local degrees of freedom. Following Pollmann and Turner [39], one can define a non-local order parameter to detect different symmetric phases of bosonic chains as

$$Z_{\mathcal{T}} = \langle \Psi | \otimes \langle \Psi | (|R_{I_1}\rangle \langle R_{I_1}|) (\text{Swap}_{I_2} |\Psi\rangle \otimes |\Psi\rangle), \quad (8)$$

where $|R_{I_1}\rangle = \prod_{k \in I_1} \left(\sum_{j_k, j'_k} U_T^{j_k, j'_k} |j_k\rangle \otimes |j'_k\rangle \right)$, and $|j\rangle$ is the j -th state in the basis for a given site. This is shown diagrammatically in Fig. 3(b) [42]. Here, we separate two regions of the chain I_1 and I_2 , apply partial time-reversal to I_1 and swap the I_2 regions of two copies of the state wave function. It is important that I_1 and I_2 are immediate neighboring regions; as we show in Appendix F, this is equivalent to creating a cross-cap in spacetime [43].

For our purposes, it is useful to rewrite Eq. (8) in a different form by using the *partial transpose* of the density

matrix

$$Z_{\mathcal{T}} = \text{tr}(\rho_I U_T^{I_1} \rho_I^{T_1} [U_T^{I_1}]^\dagger), \quad (9)$$

which can also be applied to fermionic systems. Here, $\rho_I = \text{tr}_{S \setminus I}(|\Psi\rangle\langle\Psi|)$ is the reduced density matrix of the part $I = I_1 \cup I_2$ of the chain S and the partial transpose is defined by

$$\rho_I^{T_1} = \sum_{ijkl} |e_i^1, e_j^2\rangle \langle e_k^1, e_l^2| \rho_I |e_i^1, e_l^2\rangle \langle e_k^1, e_j^2|, \quad (10)$$

where $|e_j^1\rangle$ and $|e_k^2\rangle$ denote an orthonormal set of states in the I_1 and I_2 regions.

Partial transpose for fermions.— To generalize the expression (9) for fermionic systems, we need to introduce a proper partial transpose for fermions. It is more convenient to expand the density matrix in the coherent state basis

$$\rho_I = \int d[\bar{\xi}, \xi] d[\bar{\chi}, \chi] |\{\bar{\xi}_j\}\rangle \rho_I(\{\bar{\xi}_j\}; \{\chi_j\}) |\{\xi_j\}\rangle \langle\{\bar{\chi}_j\}|,$$

where $d[\bar{\xi}, \xi] = \prod_i d\bar{\xi}_i d\xi_i e^{-\sum_j \bar{\xi}_j \xi_j}$ and $\rho_I(\{\bar{\xi}_j\}; \{\chi_j\}) = \langle\{\bar{\xi}_j\} | \rho_I | \{\chi_j\}\rangle$. Using the transformation rules for constructing a time-reversal cross-cap in the path integral formalism (Eq. (5)), the analog of Eq. (10) for fermions can be defined as

$$\begin{aligned} U_T^{I_1} \rho_I^{T_1} [U_T^{I_1}]^\dagger &:= \int d[\bar{\xi}, \xi] d[\bar{\chi}, \chi] |\{-i\bar{\chi}_j\}_{j \in I_1}, \{\xi_j\}_{j \in I_2}\rangle \\ &\times \rho_I(\{\bar{\xi}_j\}; \{\chi_j\}) \langle\{-i\xi_j\}_{j \in I_1}, \{\bar{\chi}_j\}_{j \in I_2}|. \end{aligned} \quad (11)$$

The change of variable is effectively equivalent to applying the time-reversal operator only to the I_1 interval. An alternative definition of the partial transpose is in terms of Majorana fermions [44]. In general, the density matrix can be written as

$$\rho_I = \sum_{\kappa, \tau}^{|\kappa| + |\tau| = \text{even}} w_{\kappa, \tau} c_{m_1}^{\kappa_1} \cdots c_{m_{2k}}^{\kappa_{2k}} c_{n_1}^{\tau_1} \cdots c_{n_{2l}}^{\tau_{2l}}, \quad (12)$$

where c_i are Majorana fermions in region $I = I_1 \cup I_2 = \{m_1, \dots, m_{2k}\} \cup \{n_1, \dots, n_{2l}\}$. We use the notation $c_x^0 = \mathbb{I}$ and $c_x^1 = c_x$, so that $\kappa_i, \tau_j \in \{0, 1\}$. We also introduce the vectors (bit strings) $\kappa = (\kappa_1, \dots, \kappa_{2k})$, $\tau = (\tau_1, \dots, \tau_{2l})$, and their norms $|\kappa| = \sum_{j=1}^{2k} \kappa_j$, $|\tau| = \sum_{j=1}^{2l} \tau_j$. The constraint $|\kappa| + |\tau| = \text{even}$ represents that ρ_I has a definite fermion parity.

The fermionic partial transpose is defined by

$$\rho_I^{T_1} := \sum_{\kappa, \tau} w_{\kappa, \tau} \mathcal{R}(c_{m_1}^{\kappa_1} \cdots c_{m_{2k}}^{\kappa_{2k}}) c_{n_1}^{\tau_1} \cdots c_{n_{2l}}^{\tau_{2l}}, \quad (13)$$

with the condition $\mathcal{R}(M_1 M_2) = \mathcal{R}(M_1) \mathcal{R}(M_2)$ for every two operators M_1 and M_2 [45]. This condition allows for

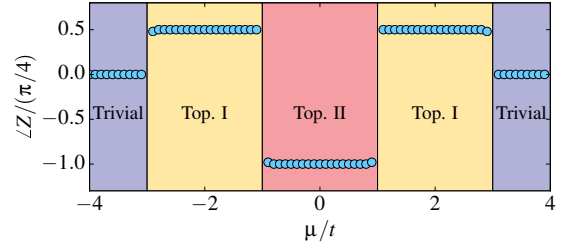


FIG. 5. SPT invariant for the three-dimensional inversion symmetric superconductor (class D), Eq. (15). Top. I (II) corresponds to the phase with odd (even) number of gapless Majorana surface states. Here, $N = 12^3$ and $N_{\text{part}} = 6^3$.

a $U(1)$ phase ambiguity which, when \mathcal{R} acts on one Majorana fermion, shows up as $\mathcal{R}(c) = e^{i\theta} c$. The definition in Eq. (11) for the time-reversal symmetry corresponds to $e^{i\theta} = \pm i$ (see Appendix F for details).

As an example, we consider the symmetry class BDI. Figure 4 shows $Z_{\mathcal{T}}$ of the Majorana chain Eq. (1) over a range of μ values. Well inside the SPT phase, $Z_{\mathcal{T}}$ is given by

$$Z_{\mathcal{T}} \sim e^{i\frac{\pi}{4}} / 2\sqrt{2}, \quad (14)$$

whereas $Z_{\mathcal{T}} \leq 1$ in the trivial phase. Therefore, partial transpose can serve as a non-local operation to obtain the complex phase of the partition function on $\mathbb{R}P^2$. (Further examples including analytical computation of $Z_{\mathcal{T}}$ for the fixed point wave function are provided in Appendix F.)

Higher dimensions.— Our scheme, illustrated so far for one-dimensional topological superconductors, can be generalized to other fermionic SPT phases, in particular to higher dimensions. As an example in three dimensions, we study the inversion symmetric topological superconductors in class D (e.g., $^3\text{He-B}$ phase). Let us consider the BdG Hamiltonian on a cubic lattice, which is given in momentum space as $\hat{H} = (1/2) \sum_{\mathbf{k}} \Psi^\dagger(\mathbf{k}) h(\mathbf{k}) \Psi(\mathbf{k})$, where $\Psi^\dagger(\mathbf{k}) = (f_\uparrow^\dagger(\mathbf{k}), f_\downarrow^\dagger(\mathbf{k}), f_\downarrow(-\mathbf{k}), -f_\uparrow(-\mathbf{k}))$, and

$$\begin{aligned} h(\mathbf{k}) &= [-t(\cos k_x + \cos k_y + \cos k_z) - \mu] \tau_z \\ &+ \Delta [\sin k_x \tau_x \sigma_x + \sin k_y \tau_x \sigma_y + \sin k_z \tau_x \sigma_z]. \end{aligned} \quad (15)$$

This model is invariant under inversion $\mathcal{I} f_\sigma(x, y, z) \mathcal{I}^{-1} = i f_\sigma(-x, -y, -z)$ (Appendix G). The relevant topological classification is given by Pin^+ bordism group in $(3+1)$ dimensions, $\Omega_4^{Pin^+} = \mathbb{Z}_{16}$, where \mathbb{Z}_{16} is generated by the four dimensional real projective space $\mathbb{R}P^4$, which is realized by making one cross-cap in S^4 [27, 33, 34, 46]. To extract the corresponding SPT invariant from the ground state $|\Psi\rangle$, we take the partial inversion $Z_{\mathcal{T}} = \langle\Psi | \mathcal{I}_{\text{part}} | \Psi\rangle$ which acts on a closed three ball. The numerically computed SPT invariant is shown in Fig. 5. It is quite remarkable that the partial inversion yields the correct \mathbb{Z}_{16} and \mathbb{Z}_8 complex phases in the topological phases characterized by odd and even number of gapless Majorana

surface modes, respectively.

Discussion.— In conclusion, we present an approach to detect interacting SPT phases by introducing a spacetime cross-cap in the path-integral. We also propose non-local order parameters, partial reflection/transposition, to detect interacting SPT phase of a given state wave function.

While we used a non-interacting clean fermionic model (the Kitaev chain (1)) to demonstrate our method, we emphasize that the SPT topological invariants introduced in this paper are applicable to interacting models and in the presence of disorder, and can be used in numerical simulations. For example, the spacetime path-integral with a cross-cap can be implemented and computed in the world-line quantum Monte Carlo. In Appendix E, we present the calculation of the SPT invariant in an interacting Majorana chain, by making use of the known exact expression of the ground state [47].

To establish the robustness of the partial reflection, we provide direct numerical calculation of the effect of chemical potential disorder in Appendix H. We observe that the partial reflection is indeed unaffected. Using the partial reflection, we also reproduce the phase diagram of the disordered Majorana chain [48, 49].

In addition, throughout this letter, we consider BCS mean-field wave functions which do not preserve the particle number. One important question is whether the partial transformation works for particle number conserving systems or not [50, 51]. In principle, to fully establish the applicability of the partial transformation one must study the ground state of an interacting model which supports topological phases. Instead, as a first step in this direction, we examine the partial reflection for projected-BCS wave functions defined by $|\Psi_{\bar{n}}\rangle = \mathcal{P}_{\bar{n}}|\Psi\rangle$ where $|\Psi\rangle$ is the ground state of the mean-field Hamiltonian in Eq. (1) and $\mathcal{P}_{\bar{n}}$ is the particle number projection operator. Using variational Monte Carlo, we find that the phase of Z remains quantized as in the mean-field wave function (Appendix I).

Acknowledgements.— We acknowledge insightful discussions with Takahiro Morimoto, Hosho Katsura and Xueda Wen. This work was supported in part by the National Science Foundation grant DMR-1455296, by the U.S. Department of Energy, Office of Science, Office of Advanced Scientific Computing Research, Scientific Discovery through Advanced Computing (SciDAC) program under Award Number FG02-12ER46875, and by Alfred P. Sloan foundation. KS is supported by JSPS Postdoctoral Fellowship for Research Abroad.

[1] M. Z. Hasan and C. L. Kane, *Rev. Mod. Phys.* **82**, 3045 (2010).
 [2] X.-L. Qi and S.-C. Zhang, *Rev. Mod. Phys.* **83**, 1057 (2011).

[3] A. P. Schnyder, S. Ryu, A. Furusaki, and A. W. W. Ludwig, *Phys. Rev. B* **78**, 195125 (2008).
 [4] S. Ryu, A. P. Schnyder, A. Furusaki, and A. W. W. Ludwig, *New Journal of Physics* **12**, 065010 (2010).
 [5] A. Kitaev, *AIP Conference Proceedings* **1134**, 22 (2009).
 [6] L. Fu, *Phys. Rev. Lett.* **106**, 106802 (2011).
 [7] C.-K. Chiu, H. Yao, and S. Ryu, *Phys. Rev. B* **88**, 075142 (2013).
 [8] T. Morimoto and A. Furusaki, *Phys. Rev. B* **88**, 125129 (2013).
 [9] K. Shiozaki and M. Sato, *Phys. Rev. B* **90**, 165114 (2014).
 [10] L. Fidkowski and A. Kitaev, *Phys. Rev. B* **81**, 134509 (2010).
 [11] L. Fidkowski and A. Kitaev, *Phys. Rev. B* **83**, 075103 (2011).
 [12] X.-L. Qi, *New J. Phys.* **15**, 065002 (2013).
 [13] S. Ryu and S.-C. Zhang, *Phys. Rev. B* **85**, 245132 (2012).
 [14] Z.-C. Gu and M. Levin, *Phys. Rev. B* **89**, 201113 (2014).
 [15] H. Yao and S. Ryu, *Phys. Rev. B* **88**, 064507 (2013).
 [16] L. Fidkowski, X. Chen, and A. Vishwanath, *Phys. Rev. X* **3**, 041016 (2013).
 [17] C. Wang, A. C. Potter, and T. Senthil, *Science* **343**, 629 (2014).
 [18] C. Wang and T. Senthil, *Phys. Rev. B* **89**, 195124 (2014).
 [19] M. A. Metlitski, L. Fidkowski, X. Chen, and A. Vishwanath, *arXiv:14063032* (2014).
 [20] Y.-Z. You and C. Xu, *Phys. Rev. B* **90**, 245120 (2014).
 [21] H. Isobe and L. Fu, *Phys. Rev. B* **92**, 081304 (2015).
 [22] C.-T. Hsieh, G. Y. Cho, and S. Ryu, *Phys. Rev. B* **93**, 075135 (2016).
 [23] T. Morimoto, A. Furusaki, and C. Mudry, *Phys. Rev. B* **92**, 125104 (2015).
 [24] A. Kapustin, *arXiv:1403.1467* (2014).
 [25] A. Kapustin, *arXiv:1404.6659* (2014).
 [26] D. S. Freed, *arXiv:1406.7278* (2014).
 [27] A. Kapustin, R. Thorngren, A. Turzillo, and Z. Wang, *Journal of High Energy Physics* **2015**, 1 (2015).
 [28] D. S. Freed and M. J. Hopkins, *arXiv:1604.06527* (2016).
 [29] X. Chen, Z.-C. Gu, Z.-X. Liu, and X.-G. Wen, *Phys. Rev. B* **87**, 155114 (2013).
 [30] Z.-C. Gu and X.-G. Wen, *Phys. Rev. B* **90**, 115141 (2014).
 [31] C.-T. Hsieh, O. M. Sule, G. Y. Cho, S. Ryu, and R. G. Leigh, *Phys. Rev. B* **90**, 165134 (2014).
 [32] G. Y. Cho, C.-T. Hsieh, T. Morimoto, and S. Ryu, *Phys. Rev. B* **91**, 195142 (2015).
 [33] E. Witten, *arXiv:1508.04715* (2015).
 [34] M. A. Metlitski, *arXiv:1510.05663* (2015).
 [35] A. M. Turner, F. Pollmann, and E. Berg, *Phys. Rev. B* **83**, 075102 (2011).
 [36] A. Y. Kitaev, *Physics-Uspekhi* **44**, 131 (2001).
 [37] In addition, to account for orientation-preserving symmetries, spacetime manifolds must be considered together with background gauge fields.
 [38] L.-X. Cen, *Phys. Rev. B* **80**, 132405 (2009).
 [39] F. Pollmann and A. M. Turner, *Phys. Rev. B* **86**, 125441 (2012).
 [40] F. Pollmann, E. Berg, A. M. Turner, and M. Oshikawa, *Phys. Rev. B* **85**, 075125 (2012).
 [41] R. M. Lutchyn, J. D. Sau, and S. Das Sarma, *Phys. Rev. Lett.* **105**, 077001 (2010).
 [42] The fact that we need two copies may be understood by considering a single site system and the overlap

$\langle \psi | \mathcal{T} | \psi \rangle = \sum_{jj'} U_T^{jj'} \psi_j^* \psi_{j'}$, where ψ_j is the amplitude of the wave function corresponding to $|j\rangle$. We see that both ψ factors appear as complex conjugates, which is different from an ordinary expectation value. A direct way to obtain such quantity is to consider the overlap between two (unentangled) copies of the system $|\psi_2\rangle = |\psi\rangle \otimes |\psi\rangle$ and the basis states $|R\rangle = \sum_{jj'} U_T^{jj'} |j\rangle \otimes |j'\rangle$. Then, $\langle \psi | \mathcal{T} | \psi \rangle = \langle \psi_2 | R \rangle$.

- [43] K. Shiozaki and S. Ryu, [arXiv:1607.06504](#) (2016).
- [44] V. Eisler and Z. Zimborás, *New Journal of Physics* **17**, 053048 (2015).
- [45] This condition is in contrast to that of Ref. [44] where $\mathcal{R}(M_1 M_2) = \mathcal{R}(M_2) \mathcal{R}(M_1)$ is considered.
- [46] R. Kirby and L. Taylor, *Geometry of low-dimensional manifolds* **2**, 177 (1990).
- [47] H. Katsura, D. Schuricht, and M. Takahashi, *Phys. Rev. B* **92**, 115137 (2015), [arXiv:1507.04444](#) [cond-mat.str-el].
- [48] I. Mondragon-Shem, T. L. Hughes, J. Song, and E. Prodan, *Phys. Rev. Lett.* **113**, 046802 (2014).
- [49] J. Song and E. Prodan, *Phys. Rev. B* **89**, 224203 (2014).
- [50] G. Ortiz, J. Dukelsky, E. Cobanera, C. Eсеbbag, and C. Beenakker, *Phys. Rev. Lett.* **113**, 267002 (2014).
- [51] G. Ortiz and E. Cobanera, [arXiv:1601.07764](#) (2016).

Supplementary information for detection of symmetry-protected topological phases in fermionic many-body systems

Hassan Shapourian, Ken Shiozaki, and Shinsei Ryu

Department of Physics, University of Illinois at Urbana-Champaign, Urbana Illinois 61801, USA

(Dated: September 28, 2016)

The supplementary information is organized as follows: Appendices A - G are devoted to explaining technical details of construction of SPT invariant from a spacetime cross-cap. In Appendix H, we discuss the effect of disorder on partial reflection in class D one-dimensional superconductors with reflection symmetry. In Appendix I, we show that the partial reflection works for the projected BCS wave function onto the sector with a fixed number of fermions.

An overview of symmetry classes, spatial dimensions, and SPT invariants introduced in the main text and appendices is outlined in Table I.

Symmetry class	Spatial dimension	Topological classification	Generating manifold	Spacetime cross-cap
D + R ₋	1	$\Omega_2^{Pin^-} = \mathbb{Z}_8$	$\mathbb{R}P^2$	Partial reflection
BDI	1	$\Omega_2^{Pin^-} = \mathbb{Z}_8$	$\mathbb{R}P^2$	Partial time inversion or adjacent partial transpose
A + R	1	$\Omega_2^{Pin^e} = \mathbb{Z}_4$	$\mathbb{R}P^2$	Partial reflection
D + I	3	$\Omega_4^{Pin^+} = \mathbb{Z}_{16}$	$\mathbb{R}P^4$	Partial inversion

TABLE I. Fermionic symmetry-protected topological phases discussed in the text. For the symmetry classes “D+R₋” and “A+R”, we follow the notation in Refs. [1–3]. Symmetry class “D+I” means symmetry class D in the presence of inversion symmetry.

CONTENTS

A. Calculation of the partition function on discretized spacetime	2
B. BdG Hamiltonian and numerical details	3
C. Partial reflection of fixed-point wave function	5
D. Fermionic matrix product states	6
E. Partial reflection: More examples	9
1. Exact ground state wave functions for interacting Majorana chains	9
2. <i>s</i> -wave construction of Majorana chain	11
3. Class A in the presence of reflection (Class A+R)	12
F. Partial transpose: More details	14
1. Partial transpose for bosonic density matrix	14
2. Partial transpose in fermionic coherent state representation	14
3. Partial transpose on fermionic operators	16
4. Fermionic matrix product state	18
5. Grassmann representation of BdG ground state	20
6. Fixed-point wave function	20
G. Three-dimensional inversion symmetric topological superconductor (Class D + inversion)	22
H. Effect of disorder on partial reflection	23
I. Partial reflection for projected wave functions	23
References	25

Appendix A: Calculation of the partition function on discretized spacetime

In this appendix, we discuss how the computation of the partition function on a discretized spacetime has been done. We also show the transformation rules of Grassmann variables which are equivalent to the action of the time-reversal and reflection symmetries. For numerical purposes, we define the partition function on a spacetime lattice as in

$$Z = \int \prod_{j=1}^{N_t} d[\xi_j] d[\bar{\xi}_j] e^{\sum_j [\bar{\xi}_{j+1} \cdot \xi_j - \bar{\xi}_j \cdot \xi_j]} e^{-\epsilon \sum_j H(\bar{\xi}_{j+1}, \xi_j)}, \quad (\text{A1})$$

where we consider a discretized time axis, $\epsilon = \beta/N_t$, and a real-space lattice where the Grassmann variables $\xi_j(x)$ and $\bar{\xi}_j(x)$ are defined on j th time slice and position x on the lattice. We use the shorthand notation $\bar{\xi}_j \cdot \xi_{j'} = \sum_x \bar{\xi}_j(x) \xi_{j'}(x)$. The Hamiltonian operator in this representation becomes a polynomial, given by

$$e^{-\epsilon H(\bar{\xi}_{j+1}, \xi_j)} = e^{-\bar{\xi}_{j+1} \xi_j} \langle \xi_{j+1} | e^{-\epsilon \hat{H}} | \xi_j \rangle. \quad (\text{A2})$$

The discretized partition function at zero temperature corresponds to the limits $\epsilon \rightarrow 0$ and $N_t \rightarrow \infty$ such that $\beta = N_t \epsilon \rightarrow \infty$.

The partition function can be computed exactly for quadratic Hamiltonians. Let us consider the Kitaev Majorana chain,

$$H(\bar{\xi}_{j+1}, \xi_j) = \sum_x (\xi_j^T(x+1) A \xi_j(x) + \xi_j^T(x) B \xi_j(x)) \quad (\text{A3})$$

where $\xi_j^T(x) = (\bar{\xi}_{j+1}(x), \xi_j(x))$ is a two-component vector (where we use the new notation $\xi_j^1 = \bar{\xi}_{j+1}$ and $\xi_j^2 = \xi_j$) and we introduce the following matrices

$$A = \begin{pmatrix} \Delta & -t \\ t & -\Delta^* \end{pmatrix} \quad (\text{A4})$$

$$B = \frac{1}{2} \begin{pmatrix} 0 & -\mu \\ \mu & 0 \end{pmatrix}. \quad (\text{A5})$$

The full partition function becomes

$$Z = \int \prod_{j=1}^{N_t} d[\xi_j] d[\bar{\xi}_j] e^{\sum_{j,x} \xi_j^T(x) [\frac{\sigma_2}{2} \sigma_2 - \epsilon B] \xi_j(x)} e^{-\epsilon \sum_{j,x} \xi_j^T(x+1) A \xi_j(x)} e^{\sum_{j,x} \xi_{j+1}^T(x) A_t \xi_j(x)} \quad (\text{A6})$$

where σ_2 is the second Pauli matrix and

$$A_t = \begin{pmatrix} 0 & 0 \\ 1 & 0 \end{pmatrix}. \quad (\text{A7})$$

The last term $\xi_{j+1}^T(x) A_t \xi_j(x) = \xi_{j+1}^2(x) \xi_j^1(x)$ is the hopping term along the time direction. Time inversion changes the time index $j \rightarrow N_t - j$. So, for the last term to be time-reversal invariant it must transform as in

$$\xi_{j+1}^2(x) \xi_j^1(x) \rightarrow i^2 \xi_{N_t-j-1}^1(x) \xi_{N_t-j}^2(x) \quad (\text{A8})$$

which implies the transformation rules

$$\xi_j^1(x) \rightarrow i \xi_{N_t-j}^2(x) \quad (\text{A9})$$

$$\xi_j^2(x) \rightarrow i \xi_{N_t-j}^1(x) \quad (\text{A10})$$

or in the matrix form

$$\xi_j(x) \rightarrow i \sigma_1 \xi_{N_t-j}(x). \quad (\text{A11})$$

Having this transformation rule, let us check whether other terms in action are invariant.

The real space hopping matrix element can be written as

$$A = -it\sigma_2 + \text{Re}[\Delta]\sigma_3 + i\text{Im}[\Delta]\sigma_0. \quad (\text{A12})$$

The Hamiltonian term is always invariant due to anticommuting property of Grassmann variables. Therefore, one can impose twisted boundary conditions across fixed position contours (vertical lines) as introduced in Eq. (6) of the main text.

The reflection symmetry can be similarly imposed on the action in Eq. (A6),

$$\xi_j(x) \rightarrow i\sigma_3\xi_j(-x). \quad (\text{A13})$$

Using this definition, one can impose twisted boundary condition across fixed time contours (horizontal lines) in the spacetime.

In either cases, the partition function in Eq. (A6) can be computed exactly in terms of a Pfaffian of discretized action matrix, since there are only on-site and hopping terms in both time and space directions.

Appendix B: BdG Hamiltonian and numerical details

In this appendix, we explain how the BCS wave functions are constructed and how the overlaps are computed. In general, the BdG Hamiltonian in the Nambu basis over real space can be written as

$$\hat{H} = \frac{1}{2} \sum_{i,j} \psi_i^\dagger \begin{pmatrix} t_{ij} & \Delta_{ij} \\ -\Delta_{ij}^* & -t_{ij}^T \end{pmatrix} \psi_j. \quad (\text{B1})$$

where the Nambu spinor is $\psi_i^\dagger = (f_i^\dagger, f_i)$, $t_{ij}^\dagger = t_{ij}$ is a Hermitian matrix and $\Delta_{ij}^\dagger = -\Delta_{ij}^*$ is a skew symmetric matrix. We diagonalize the Hamiltonian to find the eigenvalues ϵ_n

$$\begin{pmatrix} t_{ij} & \Delta_{ij} \\ -\Delta_{ij}^* & -t_{ij}^T \end{pmatrix} \begin{pmatrix} u_{jn} \\ v_{jn} \end{pmatrix} = \epsilon_n \begin{pmatrix} u_{in} \\ v_{in} \end{pmatrix}, \quad (\text{B2})$$

where n is energy eigenvalue index and i, j refer to the sites on the lattice. Taking the complex conjugate of the above expression and exchange the rows yield

$$\begin{pmatrix} t_{ij} & \Delta_{ij} \\ -\Delta_{ij}^* & -t_{ij}^T \end{pmatrix} \begin{pmatrix} v_{jn}^* \\ u_{jn}^* \end{pmatrix} = -\epsilon_n \begin{pmatrix} v_{jn}^* \\ u_{jn}^* \end{pmatrix}. \quad (\text{B3})$$

We define the Bogoliubov operators

$$\begin{pmatrix} b_n \\ b_n^\dagger \end{pmatrix} = \begin{pmatrix} u_{in}^* & v_{in}^* \\ u_{in} & v_{in} \end{pmatrix} \begin{pmatrix} f_i \\ f_i^\dagger \end{pmatrix} \quad (\text{B4})$$

where sum over i is assumed and the inverse relation

$$\begin{pmatrix} f_i \\ f_i^\dagger \end{pmatrix} = \begin{pmatrix} u_{in} & v_{in}^* \\ v_{in} & u_{in}^* \end{pmatrix} \begin{pmatrix} b_n \\ b_n^\dagger \end{pmatrix} \quad (\text{B5})$$

here, sum over n is assumed.

The Hamiltonian in this new basis reads

$$H = \sum_n \epsilon_n (b_n^\dagger b_n - \frac{1}{2}). \quad (\text{B6})$$

Assuming all $\epsilon_n > 0$, the ground state wave function must obey the condition $b_n |\Psi\rangle = 0$. This means that

$$(u_{in}^* f_i + v_{in}^* f_i^\dagger) |\Psi\rangle = 0, \quad (\text{B7})$$

where sum over repeated index i is assumed. The ground state wave function can then be written as

$$|\Psi\rangle = \exp\left(\frac{1}{2}\sum_{i,j}\phi_{ij}f_i^\dagger f_j^\dagger\right)|0\rangle, \quad (\text{B8})$$

where

$$\phi_{ij} = v_{in}^*[u^*]_{nj}^{-1}. \quad (\text{B9})$$

Let us check that this wave function satisfies Eq. (B7).

$$\begin{aligned} (u_{in}^*f_i + v_{in}^*f_i^\dagger)|\Psi\rangle &= (u_{in}^*f_i + v_{in}^*f_i^\dagger)\exp\left(\frac{1}{2}\sum_{i,j}\phi_{ij}f_i^\dagger f_j^\dagger\right)|0\rangle \\ &= \exp\left(\frac{1}{2}\sum_{i,j}\phi_{ij}f_i^\dagger f_j^\dagger\right)(u_{in}^*(f_i - \phi_{li}f_l^\dagger) + v_{in}^*f_i^\dagger)|0\rangle \\ &= \exp\left(\frac{1}{2}\sum_{i,j}\phi_{ij}f_i^\dagger f_j^\dagger\right)(u_{in}^*f_i - u_{in}^*[u^*]_{mi}^{-1}v_{lm}^*f_l^\dagger + v_{in}^*f_i^\dagger)|0\rangle \\ &= 0, \end{aligned} \quad (\text{B10})$$

where we use the identity

$$\exp\left(-\frac{1}{2}\sum_{i,j}\phi_{ij}f_i^\dagger f_j^\dagger\right)f_i\exp\left(\frac{1}{2}\sum_{i,j}\phi_{ij}f_i^\dagger f_j^\dagger\right) = f_i - \phi_{li}f_l^\dagger. \quad (\text{B11})$$

One difficulty with the wave function in Eq. (B8) is that if pairing vanishes at any point in the Brillouin zone u_{jn} becomes singular and not invertible. These are simply due to fully occupied states which cannot be represented as a particle-hole mixture (BCS-type wave function).

The inner product of two wave functions in the form of Eq. (B8) is

$$\langle\Psi_1|\Psi_2\rangle = \left[\det(\mathbf{1} + \phi_1^\dagger \cdot \phi_2)\right]^{1/2}, \quad (\text{B12})$$

which can also be written as

$$\langle\Psi_1|\Psi_2\rangle = \det\left[\left(\begin{array}{c} u_1^* \\ v_1^* \end{array}\right)^\dagger \cdot \left(\begin{array}{c} u_2^* \\ v_2^* \end{array}\right)\right]^{1/2}. \quad (\text{B13})$$

The second expression does not involve inverting v_i matrices and hence more efficient.

It is important to note that the definition in Eq. (B8) can be used to write wave function with a fixed number of particles. We apply a projection operator \mathcal{P}_n to the BCS wave function in Eq. (B8)

$$|\Psi_n\rangle = \mathcal{P}_n|\Psi\rangle, \quad (\text{B14})$$

to project out all other particle numbers. This implies that for a particle number sector with n particles at positions $\{r_1, \dots, r_n\}$ the wave function can be written as

$$\begin{aligned} \Psi_n(r_1, \dots, r_n) &= \langle r_1, \dots, r_n | \mathcal{P}_n | \Psi \rangle \\ &= \text{Pf}[\phi_{ij}(r_1, \dots, r_n)] \end{aligned} \quad (\text{B15})$$

where the indices i and j refer to the real-space positions, i.e., the corresponding rows and columns of ϕ_{ij} , i.e. $i, j \in \{r_1, \dots, r_n\}$, must be chosen.

Appendix C: Partial reflection of fixed-point wave function

In this appendix, we write down the explicit form of the fixed-point Majorana chain Hamiltonian and its ground state wave function and analytically derive the partial reflection in this case. In the Majorana basis, the Majorana chain Hamiltonian (Eq. (1) of main text) takes the form

$$\hat{H} = \frac{i}{2} \sum_{x=1}^N [(\Delta + t)c_x^R c_{x+1}^L + (\Delta - t)c_x^L c_{x+1}^R] - \frac{\mu}{2} \sum_x (1 + ic_x^L c_x^R), \quad (\text{C1})$$

which is derived by the following substitutions in the original Hamiltonian,

$$f_x^\dagger = \frac{e^{-i\phi/2}}{2}(c_x^L - ic_x^R), \quad f_x = \frac{e^{i\phi/2}}{2}(c_x^L + ic_x^R). \quad (\text{C2})$$

From now on, we take Δ to be real ($\phi = 0$) for simplicity, while the result does not depend on this choice of the gauge. The fixed-point limit (zero correlation length) is defined when $\Delta = t$ and $\mu = 0$. In this limit, the Hamiltonian reads

$$H = i \sum_{x=1}^{N-1} c_x^R c_{x+1}^L \quad (\text{C3})$$

$$= \sum_{x=1}^{N-1} (2g_x^\dagger g_x - 1) \quad (\text{C4})$$

where the new fermion operators are

$$g_x = \frac{1}{2}(c_x^R + ic_{x+1}^L) = \frac{i}{2}(f_x^\dagger - f_x + f_{x+1}^\dagger + f_{x+1}), \quad (\text{C5})$$

$$g_x^\dagger = \frac{1}{2}(c_x^R - ic_{x+1}^L) = \frac{i}{2}(f_x^\dagger - f_x - f_{x+1}^\dagger - f_{x+1}), \quad (\text{C6})$$

and their inverses are

$$c_x^R = g_x + g_x^\dagger, \quad c_{x+1}^L = i(g_x^\dagger - g_x). \quad (\text{C7})$$

The ground state can be found easily using the Hamiltonian in Eq. (C4), by requiring that $g_x |\Psi\rangle = 0$ which is the vacuum of g_x operators. Therefore, the wave function can be written in terms of

$$\begin{aligned} |\Psi_\pm\rangle &= \prod_{x=1}^N (1 \pm f_x^\dagger) |0\rangle \\ &= (1 \pm f_1^\dagger)(1 \pm f_2^\dagger) \dots (1 \pm f_N^\dagger) |0\rangle, \end{aligned} \quad (\text{C8})$$

where we assume the convention in which the fermion index is in ascending order. It is easy to check that $g_x |\Psi_\pm\rangle = 0$ for $1 \leq x < N$. It is worth noting that in the wave functions above $|0\rangle$ refers to the vacuum of f_x operators; i.e., $f_x |0\rangle = 0$. This means that for a given Majorana link between the sites x and $x+1$, we simply multiply the vacuum $|0\rangle$ by the operator $(1 \pm f_x^\dagger)(1 \pm f_{x+1}^\dagger)$. However, these wave functions need to be modified to account for the last link between the end sites N and 1 . In the case of an open chain, $g_N^\dagger g_N$ is absent; thus, $|\Psi_+\rangle$ and $|\Psi_-\rangle$ are degenerate. For the periodic boundary condition (PBC), the ground state wave function must be additionally annihilated by g_N operator. Thus, we have

$$\begin{aligned} |\Psi_r\rangle &= g_N |\Psi_+\rangle \\ &= (f_N^\dagger - f_N + f_1^\dagger + f_1)(1 + f_1^\dagger)(1 + f_2^\dagger) \dots (1 + f_N^\dagger) |0\rangle \\ &= |\Psi_+\rangle - |\Psi_-\rangle \\ &= \frac{1}{2^{(N-1)/2}} \prod_{x=1}^N (1 + f_x^\dagger) \Big|_{n \in \text{odd}} |0\rangle \end{aligned} \quad (\text{C9})$$

which means only terms with odd number of fermions survive. Thus, the ground state of the PBC $|\Psi_r\rangle$ has odd fermion parity. The anti-periodic boundary condition (APBC) must contain g_N mode, since the Hamiltonian term is $-g_N^\dagger g_N$. Hence, it is

$$\begin{aligned} |\Psi_{ns}\rangle &= g_N^\dagger |\Psi_+\rangle \\ &= (f_N - f_N^\dagger + f_1^\dagger + f_1)(1 + f_1^\dagger)(1 + f_2^\dagger) \dots (1 + f_N^\dagger) |0\rangle \\ &= |\Psi_+\rangle + |\Psi_-\rangle \\ &= \frac{1}{2^{(N-1)/2}} \prod_{x=1}^N (1 + f_x^\dagger) \Big|_{n \in \text{even}} |0\rangle \end{aligned} \quad (\text{C10})$$

which means it has even fermion parity.

Let us now compute the partial reflection for the even sector $|\Psi_{ns}\rangle$. The same derivation can be carried out for the odd sector. Consider a chain with N sites in total and N_{part} sites in the subsystem (we take N_{part} to be even which means reflection with respect to the central link). For simplicity we choose the sites 1 to N_{part} to be in the subsystem. The wave function (Eq. (C10)) can be rewritten as

$$|\Psi_{ns}\rangle = \frac{1}{2^{(N-1)/2}} (1 + f_1^\dagger) F_{in}^\dagger (1 + f_{N_{\text{part}}}^\dagger) F_{out}^\dagger \Big|_{n \in \text{even}} |0\rangle \quad (\text{C11})$$

$$\begin{aligned} &= \frac{1}{2^{(N-1)/2}} [(1 + f_1^\dagger f_{N_{\text{part}}}^\dagger) F_{in}^{(e)\dagger} F_{out}^{(e)\dagger} + (1 - f_1^\dagger f_{N_{\text{part}}}^\dagger) F_{in}^{(o)\dagger} F_{out}^{(o)\dagger}] |0\rangle \\ &+ \frac{1}{2^{(N-1)/2}} [(f_1^\dagger + f_{N_{\text{part}}}^\dagger) F_{in}^{(e)\dagger} F_{out}^{(o)\dagger} + (f_1^\dagger - f_{N_{\text{part}}}^\dagger) F_{in}^{(o)\dagger} F_{out}^{(e)\dagger}] |0\rangle \end{aligned} \quad (\text{C12})$$

We define the new operators

$$\begin{aligned} F_{in}^{(o/e)\dagger} &= \prod_{j=2}^{N_{\text{part}}-1} (1 + f_j^\dagger) \Big|_{n \in \text{odd/even}} \\ F_{out}^{(o/e)\dagger} &= \prod_{j=N_{\text{part}}+1}^N (1 + f_j^\dagger) \Big|_{n \in \text{odd/even}} \end{aligned} \quad (\text{C13})$$

The partial reflection is defined by

$$\mathcal{R}_{\text{part}} f_j^\dagger \mathcal{R}_{\text{part}}^{-1} = i f_{N_{\text{part}}-(j-1)}^\dagger. \quad (\text{C14})$$

Note that

$$\begin{aligned} \langle 0 | F_{in}^{(o)} \mathcal{R}_{\text{part}} F_{in}^{(o)\dagger} | 0 \rangle &= i 2^{N_{\text{part}}-3}, \\ \langle 0 | F_{in}^{(e)} \mathcal{R}_{\text{part}} F_{in}^{(e)\dagger} | 0 \rangle &= 2^{N_{\text{part}}-3}. \end{aligned} \quad (\text{C15})$$

So, we can simplify the expression for the partial reflection,

$$Z_N = \langle \Psi_{ns} | \mathcal{R}_{\text{part}} | \Psi_{ns} \rangle = \frac{1}{2^N} [2 \cdot 2^{N_{\text{part}}-3} 2^{N-N_{\text{part}}} (1+i) + 2 \cdot 2^{N_{\text{part}}-3} 2^{N-N_{\text{part}}} i(1-i)]. \quad (\text{C16})$$

Hence, we conclude

$$Z_N = \frac{1+i}{2}. \quad (\text{C17})$$

Appendix D: Fermionic matrix product states

In this appendix, we review the fermionic matrix product state [4] and show that the partial reflection gives the \mathbb{Z}_8 classification as expected for the symmetry class D with reflection. Following Dubail and Read in [4], we write an

MPS representation for a fermionic wave function is in terms of Gaussian integrals over Grassmann variables,

$$|\Psi\rangle = \int d[\xi] e^{\sum_x \xi^T(x) B \xi(x)} e^{\sum_x \xi^T(x+1) A \xi(x)} e^{\sum_x \xi^T(x) \kappa f_x^\dagger} |0\rangle \quad (\text{D1})$$

where $\xi_j^T(x) = (\xi^1(x), \xi^2(x))$ is a two-component Grassmann vector,

$$A = \begin{pmatrix} 1 & \lambda \\ -\lambda & -1 \end{pmatrix}, \quad (\text{D2})$$

$$B = \begin{pmatrix} 0 & -\lambda \\ \lambda & 0 \end{pmatrix}, \quad (\text{D3})$$

and $\kappa^T = (\kappa_1, 0)$. So, the wave function can be written in momentum space as

$$|\Psi\rangle = \int d[\xi] e^{\sum_k \xi_{-k}^T S_k \xi_k} e^{\sum_k \xi_{-k}^T \kappa f_k^\dagger} |0\rangle \quad (\text{D4})$$

where

$$S_k = \begin{pmatrix} -i \sin k & -\lambda(1 - \cos k) \\ \lambda(1 - \cos k) & i \sin k \end{pmatrix}, \quad (\text{D5})$$

and the Fourier components are defined by $\xi_k = \frac{1}{\sqrt{N}} \sum_x e^{-ikx} \xi_x$ and $f_k = \frac{1}{\sqrt{N}} \sum_x e^{ikx} f_x$. Integrating ξ_k fields (with anti-periodic boundary condition) leads to

$$|\Psi_{ns}\rangle \propto \exp\left(\sum_{k>0} g_k f_k^\dagger f_{-k}^\dagger\right) |0\rangle \quad (\text{D6})$$

in which

$$g_k = \frac{\kappa_1^2}{2} [S_k^{-1}]_{11} = \frac{\kappa_1^2}{2} \frac{i \sin k}{\sin^2 k + \lambda^2(1 - \cos k)^2}. \quad (\text{D7})$$

This is the familiar BCS wave function. However, we should note that the coefficient g_k is not exactly the same as that of the ground state of the BdG Hamiltonian, which is

$$g_k = \frac{i2\Delta \sin k}{-(2t \cos k + \mu) + \sqrt{(2t \cos k + \mu)^2 + 4\Delta^2 \sin^2 k}}. \quad (\text{D8})$$

Nevertheless, the fermionic MPS defined here is topologically non-trivial and can be used to benchmark the calculations of the partial reflection. In particular, $\lambda = 1$ and $\kappa_1 = 2$ corresponds to the fixed-point limit of the BdG Hamiltonian (with $\mu = 0$ and $t = \Delta$) where

$$g_k = i \cot \frac{k}{2}. \quad (\text{D9})$$

To compute the expectation values, we use the following definition for the complex conjugate wave function

$$\begin{aligned} \langle \Psi | \equiv (|\Psi\rangle)^\dagger &= \int d[\xi] \langle 0 | e^{\sum_x f_x \kappa^T \xi(x)} e^{\sum_x \xi^T(x) B^\dagger \xi(x)} e^{\sum_x \xi^T(x) A^\dagger \xi(x+1)} \\ &= \int d[\xi] \langle 0 | e^{\sum_x f_x \kappa^T \xi(x)} e^{\sum_x \xi^T(x) B^\dagger \xi(x)} e^{\sum_x \xi^T(x+1) (-A^*) \xi(x)} \end{aligned} \quad (\text{D10})$$

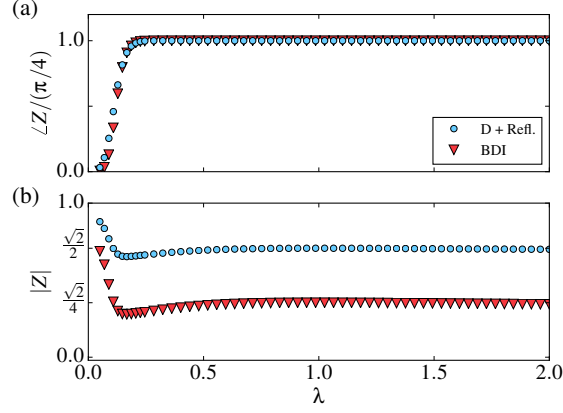


FIG. 1. Partial reflection Eq. (8) and partial transpose Eq. (10) for the fermionic MPS (Eq. (D1)). We set $\kappa_1 = 2$. The total number of sites is $N = 120$ and length of transformed subsystem is $N_{\text{part}} = 60$. For partial transpose, each I_1 and I_2 has 30 sites.

Therefore, the wave function overlap (“zero-temperature partition function”) is found by

$$\begin{aligned}
 \langle \Psi | \Psi \rangle &= \int d[\xi] \int d[\eta] e^{\sum_x \eta^T(x) B^\dagger \eta(x) + \sum_x \eta^T(x+1) (-A^*) \eta(x)} e^{\sum_x \xi^T(x) B \xi(x) + \sum_x \xi^T(x+1) A \xi(x)} e^{-\sum_x \xi^T(x) \kappa \kappa^T \eta(x)} \\
 &= \int d[\xi] \int d[\eta] \exp \left[(\xi^T, \eta^T) Y \begin{pmatrix} \xi \\ \eta \end{pmatrix} \right] \\
 &= \text{Pf}[Y]
 \end{aligned} \tag{D11}$$

where in the last line, we carry out the integrals over the Grassmann variables. The matrices are given by

$$Y = \begin{pmatrix} M & -K \\ K^T & M^\dagger \end{pmatrix} \tag{D12}$$

in which M defines the hopping between similar sites (ξ or η),

$$M = \begin{pmatrix} B & A/2 & & & -A/2 \\ -A/2 & B & A/2 & & \\ & -A/2 & B & A/2 & \\ & & \ddots & \ddots & \ddots \\ A/2 & & & -A/2 & B & A/2 \\ & & & & -A/2 & B \end{pmatrix}, \tag{D13}$$

and K denotes the link between ξ and η variables over physical degrees of freedom,

$$K = \frac{1}{2} \begin{pmatrix} \kappa \kappa^T & & & & \\ & \kappa \kappa^T & & & \\ & & \ddots & & \\ & & & \ddots & \\ & & & & \kappa \kappa^T \end{pmatrix}. \tag{D14}$$

Here, the empty matrix entries are zero.

The full reflection operator acts only on the fermion operators $\mathcal{R} f_x \mathcal{R}^{-1} = i f_{-x}$, hence, we have

$$\mathcal{R} |\Psi\rangle = \int d[\xi] e^{\sum_x \xi^T(x) B \xi(x)} e^{\sum_x \xi^T(x+1) A \xi(x)} e^{-i \sum_x \xi^T(-x) \kappa f_x^\dagger} |0\rangle. \tag{D15}$$

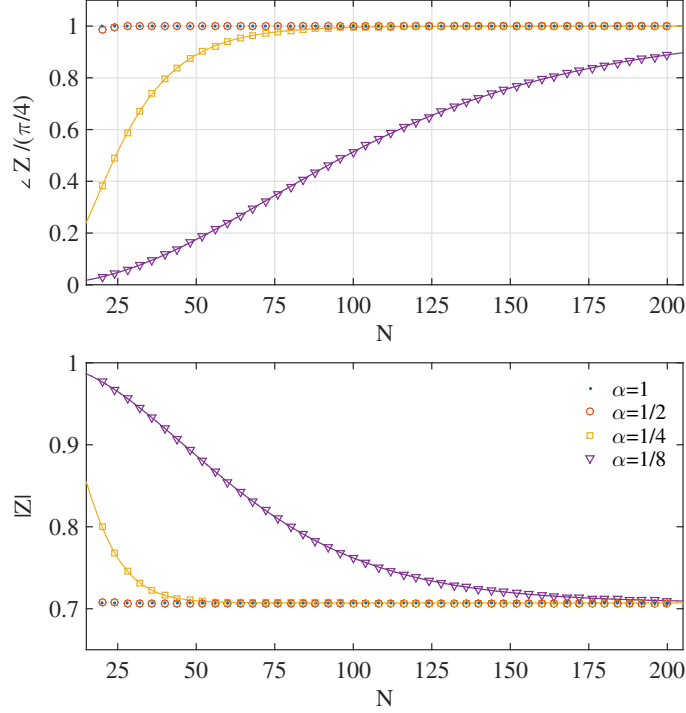


FIG. 2. Partial reflection for the interacting wave function Eq. (E2) as a function of total number of sites $N = 2N_{\text{part}}$ for various values of α . $\alpha = 1$ corresponds to the non-interacting fixed-point wave function. Solid lines show analytical expression found in Eq. (E10).

for parameter values satisfying the condition $\mu = 4\sqrt{U^2 + tU + (t^2 - \Delta^2)/4}$ can be written in a closed form as

$$|\Psi_{r(ns)}\rangle = |\Psi_+\rangle \mp |\Psi_-\rangle, \quad (\text{E2})$$

where

$$\begin{aligned} |\Psi_{\pm}^{\alpha}\rangle &= \frac{1}{(1 + \alpha^2)^{N/2}} \prod_{x=1}^N (1 \pm \alpha f_x^{\dagger}) |0\rangle \\ &= \frac{1}{(1 + \alpha^2)^{N/2}} e^{\pm \alpha f_1^{\dagger}} e^{\pm \alpha f_2^{\dagger}} \dots e^{\pm \alpha f_N^{\dagger}} |0\rangle, \end{aligned} \quad (\text{E3})$$

corresponding to odd (even) fermion parity sectors associated with (anti-)periodic boundary condition where $\alpha = \sqrt{\cot(\theta/2)}$ and $\theta = \arctan(2\Delta/\mu)$. Using the fact that the two representations of the fixed-point wave function in Eqs. (C10) and (D1) with $\lambda = 1$ and $\kappa_1 = 2$ are identical (see also [6]), it is clear that the interacting wave function given above in Eq. (E2) is equal to the MPS wave function in Eq. (D6) with $\kappa_1 = 2\alpha$. Therefore, we can use our MPS construction of the partial reflection to extract \mathbb{Z}_8 phase for generic cases where $\kappa_1 \neq 2$. Figure 2 shows the partial reflection as a function of total number of sites. It is quite remarkable that as we approach the long-chain limit (compared to the correlation length), the amplitudes and complex phases of all various cases converge to the anticipated values $1/\sqrt{2}$ and $\pi/4$, respectively. In the following, we provide an analytical derivation of this result.

We prove our result for the case with anti-periodic boundary condition. A similar derivation can be carried out for the case of periodic boundary condition. Consider a long chain with N sites in total and N_{part} sites in the subsystem such that $N = 2N_{\text{part}}$ (we take N_{part} to be even which means reflection with respect to the central link). The wave function is given by

$$|\Psi_{ns}\rangle = \frac{1}{\sqrt{\mathcal{A}_+(N)}} \prod_{x=1}^N (1 + \alpha f_x^{\dagger}) \Big|_{n \in \text{even}} |0\rangle \quad (\text{E4})$$

where the normalization factor is

$$\mathcal{A}_{\pm}(n) = \frac{1}{2}[(1 + \alpha^2)^n \pm (1 - \alpha^2)^n]. \quad (\text{E5})$$

For simplicity we choose the sites 1 to N_{part} to be in the subsystem. The wave function can be rewritten as

$$\begin{aligned} |\Psi_{ns}\rangle &= \frac{1}{\sqrt{\mathcal{A}(N)}} (1 + \alpha f_1^\dagger) F_{in}^\dagger (1 + \alpha f_{N_{\text{part}}}^\dagger) F_{out}^\dagger \Big|_{n \in \text{even}} |0\rangle \\ &= \frac{1}{\sqrt{\mathcal{A}(N)}} [(1 + \alpha^2 f_1^\dagger f_{N_{\text{part}}}^\dagger) F_{in}^{(e)\dagger} F_{out}^{(e)\dagger} + (1 - \alpha^2 f_1^\dagger f_{N_{\text{part}}}^\dagger) F_{in}^{(o)\dagger} F_{out}^{(o)\dagger}] |0\rangle \\ &\quad + \frac{\alpha}{\sqrt{\mathcal{A}(N)}} [(f_1^\dagger + f_{N_{\text{part}}}^\dagger) F_{in}^{(e)\dagger} F_{out}^{(o)\dagger} + (f_1^\dagger - f_{N_{\text{part}}}^\dagger) F_{in}^{(o)\dagger} F_{out}^{(e)\dagger}] |0\rangle. \end{aligned} \quad (\text{E6})$$

We define the new operators

$$\begin{aligned} F_{in}^{(o/e)\dagger} &= \prod_{j=2}^{N_{\text{part}}-1} (1 + \alpha f_j^\dagger) \Big|_{n \in \text{odd/even}}, \\ F_{out}^{(o/e)\dagger} &= \prod_{j=N_{\text{part}}+1}^N (1 + \alpha f_j^\dagger) \Big|_{n \in \text{odd/even}}. \end{aligned} \quad (\text{E7})$$

The partial reflection is defined by

$$\mathcal{R}_{\text{part}} f_j^\dagger \mathcal{R}_{\text{part}}^{-1} = i f_{N-(j-1)}^\dagger. \quad (\text{E8})$$

Note that

$$\begin{aligned} \langle 0 | F_{in}^{(o)} \mathcal{R}_{\text{part}} F_{in}^{(o)\dagger} | 0 \rangle &= i \mathcal{A}_-(N_{\text{part}} - 2), \\ \langle 0 | F_{in}^{(o)} \mathcal{R}_{\text{part}} F_{in}^{(o)\dagger} | 0 \rangle &= \mathcal{A}_+(N_{\text{part}} - 2). \end{aligned} \quad (\text{E9})$$

So, we have

$$\begin{aligned} Z_N = \langle \Psi_{ns} | \mathcal{R}_{\text{part}} | \Psi_{ns} \rangle &= \frac{1}{\mathcal{A}(N)} [(1 + \alpha^4) \mathcal{A}_+(N_{\text{part}} - 2) \mathcal{A}_+(N - N_{\text{part}}) + i(1 + \alpha^4) \mathcal{A}_-(N_{\text{part}} - 2) \mathcal{A}_-(N - N_{\text{part}})] \\ &\quad + \frac{2\alpha^2}{\mathcal{A}(N)} [i \mathcal{A}_+(N_{\text{part}} - 2) \mathcal{A}_-(N - N_{\text{part}}) + \mathcal{A}_-(N_{\text{part}} - 2) \mathcal{A}_+(N - N_{\text{part}})] \end{aligned} \quad (\text{E10})$$

In the thermodynamic limit $N \rightarrow \infty$, this becomes

$$\begin{aligned} \lim_{N \rightarrow \infty} Z_N &= \frac{(1 + \alpha^2)^{N-2}}{2(1 + \alpha^2)^N} [(1 + \alpha^4)(1 + i) + 2\alpha^2(i + 1)] \\ &= \frac{1 + i}{2}, \end{aligned} \quad (\text{E11})$$

where we use the fact that

$$\lim_{n \rightarrow \infty} \mathcal{A}_{\pm}(n) = \frac{1}{2}(1 + \alpha^2)^n. \quad (\text{E12})$$

Figure 2 shows the perfect agreement between analytical results and numerical calculations.

2. *s*-wave construction of Majorana chain

As another application of the partial reflection, we study the *s*-wave superconducting nanowire with spin-orbit coupling in the presence of Zeeman field which is proposed as an experimental realization of the Majorana chain [7]. This model is a member of symmetry class D and is equipped with the reflection symmetry. Hence, the interacting

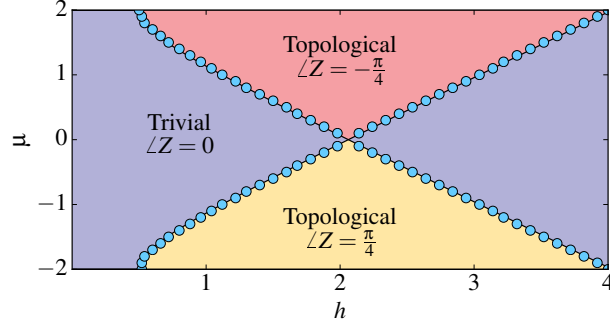


FIG. 3. Phase diagram of s -wave superconducting nanowire with spin-orbit coupling (Eq. (E13)) using the partial reflection. The boundary between a topological phase and a trivial phase is identified by a jump in $\angle Z$ from $\pm\pi/4$ to 0. The solid lines show the analytically computed phase boundaries. Here, we set $t = 1$ and $\Delta = \lambda = 0.5$. The size of total system and subsystem are $N = 200$ and $N_{\text{part}} = 100$, respectively.

classification is \mathbb{Z}_8 . The Hamiltonian is defined by

$$\begin{aligned}
 \hat{H} = & -t \sum_{x,\sigma} [f_{x+1\sigma}^\dagger f_{x\sigma} + \text{H.c.}] - \mu \sum_{x,\sigma} f_{x\sigma}^\dagger f_{x\sigma} \\
 & + \Delta \sum_x [f_{x\uparrow}^\dagger f_{x\downarrow}^\dagger + \text{H.c.}] + h_z \sum_{x,\sigma,\sigma'} (s_z)_{\sigma\sigma'} f_{x\sigma}^\dagger f_{x\sigma'} \\
 & + \lambda \sum_x [f_{x+1\uparrow}^\dagger f_{x\downarrow} - f_{x-1\uparrow}^\dagger f_{x\downarrow} + \text{H.c.}].
 \end{aligned} \tag{E13}$$

Here, the reflection symmetry acts on fermion operators as $\mathcal{R}f_{x\sigma}\mathcal{R}^{-1} = i(s_z)_{\sigma\sigma'}f_{-x\sigma'}$ where s_z is the third Pauli matrix in the spin basis. We use the partial reflection to characterize each phase and map out the phase diagram as shown in Fig. 3. The phase boundaries are accurately determined. Interestingly, the sign of the topological phase $\pm\pi/4$ at negative (positive) μ correctly captures the two distinct topological phases associated with $\nu = \pm 1$ corresponding to two chains with opposite unpaired Majorana modes on each end.

3. Class A in the presence of reflection (Class A+R)

Here, we illustrate how the partial reflection can be implemented for class A topological insulators with reflection symmetry. The topological classification is given by the Pin^c bordism in (1+1)d, that is $\Omega_2^{Pin^c} = \mathbb{Z}_4$, where \mathbb{Z}_4 is generated by the real projective plane $\mathbb{R}P^2$. We show that by means of the partial reflection we can compute the corresponding topological invariant, both numerically for a wide range of parameters and analytically for the fixed-point wave function.

As a generating model of this symmetry class, we consider the Su-Schrieffer-Heeger (SSH) model in the presence of the reflection symmetry,

$$\hat{H} = -t_2 \sum_x (f_{x+1}^{L\dagger} f_x^R + \text{H.c.}) - t_1 \sum_x (f_x^{L\dagger} f_x^R + \text{H.c.}) \tag{E14}$$

where there are two fermion species living on each site f_x^L and f_x^R . This Hamiltonian is symmetric under the reflection which acts on the fermion operators as

$$\mathcal{R}f_x^L\mathcal{R}^{-1} = if_{-x}^R, \quad \mathcal{R}f_x^R\mathcal{R}^{-1} = if_{-x}^L. \tag{E15}$$

This model realizes two topologically distinct phases: Topologically non-trivial phase for $t_2 > t_1$, where the open chain has localized fermion modes at the boundaries, and trivial phase for $t_2 < t_1$ which is just an insulator with no boundary mode. Figure 4 shows the complex phase and the amplitude of the partial reflection. Therefore, in the

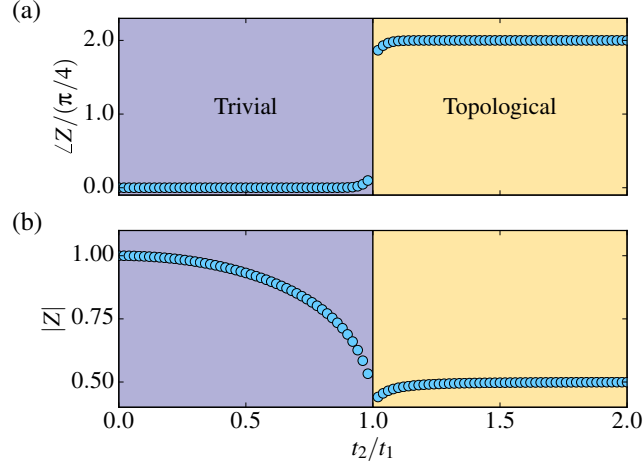


FIG. 4. Partial reflection for the SSH model. Here, $N = 200$ and $N_{\text{part}} = 100$.

topological phase we have

$$\langle \Psi | \mathcal{R}_{\text{part}} | \Psi \rangle = \frac{e^{i\frac{\pi}{2}}}{2}, \quad (\text{E16})$$

whereas in the trivial phase, we get

$$\langle \Psi | \mathcal{R}_{\text{part}} | \Psi \rangle \leq 1. \quad (\text{E17})$$

This result is consistent with \mathbb{Z}_4 classification according to the bordism theory.

Let us now show this result explicitly for the fixed-point wave function when $t_1 = 0$. The ground state is given by

$$|\Psi\rangle = \frac{1}{2^{(N+2)/2}} (f_0^{R\dagger} + f_1^{L\dagger})(f_1^{R\dagger} + f_2^{L\dagger}) \dots (f_N^{R\dagger} + f_{N+1}^{L\dagger})(f_{N+1}^{R\dagger} + f_0^{L\dagger}) |0\rangle \quad (\text{E18})$$

where we assume ascending order for the fermion indices and take N to be even (hence, the reflection is with respect to the central bond of the subsystem). We define the subsystem as the sites 1 to N . We should note that more sites can be included between the sites 0 and $N + 1$, but they do not change the final result as there is no entanglement between the subsystem and such extra sites. The ground state wave function can be rewritten as

$$|\Psi\rangle = \frac{1}{2^{(N+2)/2}} (f_0^{R\dagger} + f_1^{L\dagger}) F_{in}^\dagger (f_N^{R\dagger} + f_{N+1}^{L\dagger})(f_{N+1}^{R\dagger} + f_0^{L\dagger}) |0\rangle \quad (\text{E19})$$

where

$$F_{in}^\dagger = (f_1^{R\dagger} + f_2^{L\dagger})(f_2^{R\dagger} + f_3^{L\dagger}) \dots (f_{N-1}^{R\dagger} + f_N^{L\dagger}). \quad (\text{E20})$$

Using the fact that

$$\langle 0 | F_{in} \mathcal{R}_{\text{part}} F_{in}^\dagger | 0 \rangle = 2^{N-1} i^{N-1} (-1)^{(N-1)(N-2)/2}, \quad (\text{E21})$$

we arrive at

$$\begin{aligned} Z_N &= \langle \Psi | \mathcal{R}_{\text{part}} | \Psi \rangle \\ &= \frac{2^{N-1} i^{N-1}}{2^{N+1}} (-1)^{(N-1)(N-2)/2} \langle 0 | (f_N^R + f_{N+1}^L)(f_0^R + f_1^L)(f_0^{R\dagger} + i f_N^{R\dagger})(f_{N+1}^{L\dagger} + i f_1^{L\dagger}) | 0 \rangle \\ &= \frac{i^{(N-1)^2}}{2} = \frac{i}{2}. \end{aligned} \quad (\text{E22})$$

The last equality holds since N is even. Therefore, we recover the \mathbb{Z}_4 classification. We should note that here the amplitude is $\frac{1}{2}$ in contrast to that of the Majorana chain which is $\frac{1}{\sqrt{2}}$. In other words, the amplitude is related to the quantum dimension of the boundary modes in the form of $\prod_j d_j^{-1}$ where d_i is the quantum dimension of the j th boundary mode.

Appendix F: Partial transpose: More details

In this appendix, we present our definition of the partial transpose for a fermionic density matrix to simulate and compute a time-reversal cross-cap in terms of wave function overlaps. The strategy of constructing the fermionic partial transpose developed in this paper is to reproduce the complex \mathbb{Z}_8 phase in the partition function of spin topological quantum field theory on real projective plane $\mathbb{R}P^2$ [8]. The resulting definition of the fermionic partial transpose differs from the one that was originally introduced in Ref. [9].

After reviewing the partial transpose of a bosonic density matrix in Sec. F 1, we define the fermionic partial transpose in the coherent state basis inspired by our construction of time-reversal cross-cap in the path integral formalism, in Sec. F 2. In Sec. F 3, we review the general form of the fermionic partial transpose in terms of Majorana operators and show that both definition using the coherent state basis and Majorana operators are equivalent as long as we fix $\theta = \pi/2$ for the complex phase in the definition of a transposed Majorana operator. After we establish our definition of the partial transpose, we examine it for the fermionic MPS (Sec. F 4) and the BdG ground state wave functions (Sec. F 5). In Sec. F 6, we analytically derive the partial transpose for the fixed-point wave function of the Majorana chain and also check that the complex phase of the partial transpose is additive as we introduce more fermion flavors. In all cases, we arrive at the \mathbb{Z}_8 classification corresponding to the symmetry class BDI.

1. Partial transpose for bosonic density matrix

Before we get into details of calculations, let us briefly review the definition of the partial transpose of a bosonic density matrix. For a bosonic system (e.g., spin chains), a reduced density matrix $\rho_I = \text{tr}_{S \setminus I}(\rho)$ of a subsystem $I = I_1 \cup I_2$ consisting of two smaller subsystems I_1 and I_2 can be written as

$$\rho_I = \sum_{ijkl} \langle e_i^1, e_j^2 | \rho_I | e_k^1, e_l^2 \rangle | e_i^1, e_j^2 \rangle \langle e_k^1, e_l^2 |, \quad (\text{F1})$$

where $|e_j^1\rangle$ and $|e_k^2\rangle$ denote orthonormal bases on the Hilbert spaces \mathcal{H}_1 and \mathcal{H}_2 corresponding to the I_1 and I_2 regions. The partial transpose of a density matrix for the subsystem I_1 is defined by exchanging the matrix elements in the subsystem I_1 as in

$$\rho_I^{T_1} = \sum_{ijkl} \langle e_k^1, e_j^2 | \rho_I | e_i^1, e_l^2 \rangle | e_i^1, e_j^2 \rangle \langle e_k^1, e_l^2 |, \quad (\text{F2})$$

which is equivalent to the following transformation on the operator basis

$$\left(|e_i^1, e_j^2\rangle \langle e_k^1, e_l^2| \right)^{T_1} = |e_k^1, e_j^2\rangle \langle e_i^1, e_l^2|. \quad (\text{F3})$$

2. Partial transpose in fermionic coherent state representation

As we have seen in the main text and Appendix A, a time-reversal cross-cap can be implemented in the spacetime path integral by rearranging the Grassmann variables and the partition function of a Majorana chain with time-reversal symmetry in the presence of a cross-cap yields the \mathbb{Z}_8 complex phase associated with the \mathbb{Z}_8 classification of class BDI (see Eqs. (6) and (7) of main text). This motivates us to adapt this procedure for the ground state wave function and define the quantity $Z_{\mathcal{T}} = \text{tr}(\rho_I U_T^{I_1} \rho_I^{T_1} [U_T^{I_1}]^\dagger)$ where $\rho_I^{T_1}$ involves the fermionic partial transpose. It is worth noting that the quantity $Z_{\mathcal{T}}$ for adjacent intervals is topologically equivalent to the partition function on $\mathbb{R}P^2$ (as depicted in Fig. 5) [10]. However, if we choose disjoint intervals, such that $I_1 \cap I_2 = \emptyset$, it becomes equivalent to the partition function over the Klein bottle [11].

In order to numerically compute $Z_{\mathcal{T}}$ for a given ground state wave function, we use the coherent state representation of fermions in terms of Grassmann variables. As we show in the following, the partial transpose can be implemented

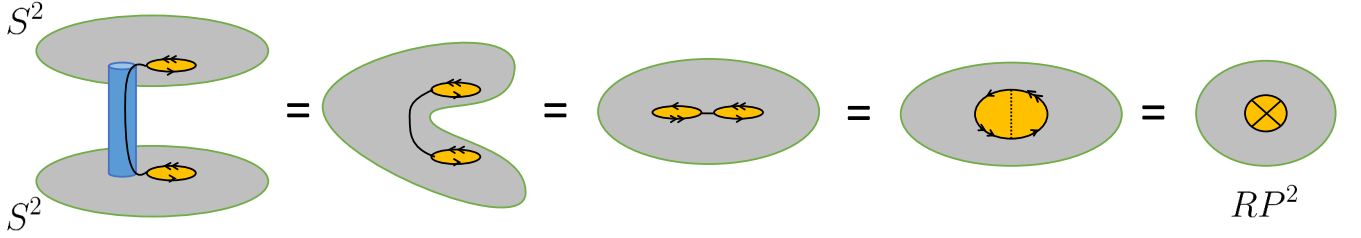


FIG. 5. Equivalence between $Z_{\mathcal{T}} = \text{tr}(\rho_I U_T^{I_1} \rho_I^{T_1} [U_T^{I_1}]^\dagger)$ and the partition function over the real projective plane RP^2 . Black lines with the same arrows are identified.

as a transformation in the space of Grassmann variables. Later, we illustrate this idea for two examples: Fermionic MPS (D1) and BdG ground state (F33). As we will see, the transformation of Grassmann variables here is very similar to that of partition function discussed in Appendix A for the partial time inversion in spacetime.

Let us begin by noting that any density matrix can be expanded in a coherent state basis as

$$\rho = \int d[\bar{\xi}]d[\xi]d[\bar{\chi}]d[\chi]e^{-\sum_j(\bar{\xi}_j\xi_j+\bar{\chi}_j\chi_j)} \langle\{\bar{\xi}_j\}|\rho|\{\chi_j\}\rangle \langle\{\xi_j\}\rangle \langle\{\bar{\chi}_j\}|, \quad (\text{F4})$$

where $\xi_j, \bar{\xi}_j, \chi_j$ and $\bar{\chi}_j$ are independent Grassmann variables which anticommute with fermion creation/annihilation operators, and $|\{\xi_j\}\rangle := e^{-\sum_j \xi_j f_j^\dagger} |0\rangle, \langle\{\bar{\chi}_j\}| := \langle 0| e^{-\sum_j f_j \bar{\chi}_j}$ are the fermionic coherent states. Note that $|\{\xi_j\}\rangle, \langle\{\bar{\chi}_j\}|$ are Grassmann even and commute with a single Grassmann variable.

Recall that for class BDI, the time-reversal symmetry (TRS) operation is defined by

$$\mathcal{T} f_j^\dagger \mathcal{T}^{-1} = f_j^\dagger, \quad \mathcal{T} i \mathcal{T}^{-1} = -i. \quad (\text{F5})$$

The TRS transformation of Grassmann variables in the path integral formalism, defined in Eq. (6) of main text, suggests that the fermionic partial transpose in the coherent basis is given by

$$U_T^{I_1} (|\{\xi_j\}_{j \in I_1}, \{\xi_j\}_{j \in I_2}\rangle \langle\{\bar{\chi}_j\}_{j \in I_1}, \{\bar{\chi}_j\}_{j \in I_2}|)^{T_1} [U_T^{I_1}]^\dagger := | \{-i\bar{\chi}_j\}_{j \in I_1}, \{\xi_j\}_{j \in I_2}\rangle \langle\{-i\xi_j\}_{j \in I_1}, \{\bar{\chi}_j\}_{j \in I_2}| \quad (\text{F6})$$

in a similar manner to (F3). Let us focus only on the combined operation (F6) at the present stage. We will discuss the operator formalism and in particular the unitary operator $U_T^{I_1}$ in Sec. F 3. There, we explain the partially transposed operator O^{T_1} where O is a generic Grassmann even operator acting on the Fock space .

It is easy to see that the definition (F6) effectively acts as a ‘‘partial transposition’’ similar to (F3) in the occupation number basis. The occupation number basis is defined by

$$|\{n_j\}_{j \in I_1}, \{n_j\}_{j \in I_2}\rangle := (f_1^\dagger)^{n_1} \dots (f_{M_1}^\dagger)^{n_{M_1}} (f_{M_1+1}^\dagger)^{n_{M_1+1}} \dots (f_N^\dagger)^{n_N} |0\rangle \quad (\text{F7})$$

for the subsystem $I = I_1 \cup I_2 = \{1, \dots, M_1\} \cup \{M_1 + 1, \dots, M\}$. For example, let us consider a two complex fermion system. The operator basis in the coherent state is

$$\begin{aligned} |\xi_1, \xi_2\rangle \langle\bar{\chi}_1, \bar{\chi}_2| &= |00\rangle \langle 00| + \bar{\chi}_1 |00\rangle \langle 10| + \bar{\chi}_2 |00\rangle \langle 01| + \bar{\chi}_1 \bar{\chi}_2 |00\rangle \langle 11| \\ &\quad - \xi_1 |10\rangle \langle 00| + \xi_1 \bar{\chi}_1 |10\rangle \langle 10| + \xi_1 \bar{\chi}_2 |10\rangle \langle 01| - \xi_1 \bar{\chi}_1 \bar{\chi}_2 |10\rangle \langle 11| \\ &\quad - \xi_2 |01\rangle \langle 00| - \bar{\chi}_1 \xi_2 |01\rangle \langle 10| + \xi_2 \bar{\chi}_2 |01\rangle \langle 01| + \bar{\chi}_1 \xi_2 \bar{\chi}_2 |01\rangle \langle 11| \\ &\quad - \xi_1 \xi_2 |11\rangle \langle 00| + \xi_1 \bar{\chi}_1 \xi_2 |11\rangle \langle 10| - \xi_1 \xi_2 \bar{\chi}_2 |11\rangle \langle 01| + \xi_1 \bar{\chi}_1 \xi_2 \bar{\chi}_2 |11\rangle \langle 11|. \end{aligned} \quad (\text{F8})$$

Thus, the transformation (F6) is given by

$$\begin{aligned}
U_T^{I_1} (|\xi_1, \xi_2\rangle \langle \bar{\chi}_1, \bar{\chi}_2|)^{T_1} [U_T^{I_1}]^\dagger &= |-i\bar{\chi}_1, \xi_2\rangle \langle -i\xi_1, \bar{\chi}_2| \\
&= |00\rangle \langle 00| + i\bar{\chi}_1 |10\rangle \langle 00| + \bar{\chi}_2 |00\rangle \langle 01| - i\bar{\chi}_1 \bar{\chi}_2 |10\rangle \langle 01| \\
&\quad - i\xi_1 |00\rangle \langle 10| + \xi_1 \bar{\chi}_1 |10\rangle \langle 10| - i\xi_1 \bar{\chi}_2 |00\rangle \langle 11| - \xi_1 \bar{\chi}_1 \bar{\chi}_2 |10\rangle \langle 11| \\
&\quad - \xi_2 |01\rangle \langle 00| + i\bar{\chi}_1 \xi_2 |11\rangle \langle 00| + \xi_2 \bar{\chi}_2 |01\rangle \langle 01| + i\bar{\chi}_1 \xi_2 \bar{\chi}_2 |11\rangle \langle 01| \\
&\quad + i\xi_1 \xi_2 |01\rangle \langle 10| + \xi_1 \bar{\chi}_1 \xi_2 |11\rangle \langle 10| - i\xi_1 \xi_2 \bar{\chi}_2 |01\rangle \langle 11| + \xi_1 \bar{\chi}_1 \xi_2 \bar{\chi}_2 |11\rangle \langle 11|. \tag{F9}
\end{aligned}$$

Comparing coefficients of these terms, the transformation (F6) can be read in the form of

$$|nm\rangle \langle nm'| \mapsto |nm\rangle \langle nm'|, \quad (n, m, m' \in \{0, 1\}). \tag{F10}$$

for the diagonal terms in the basis of the first fermion and in the following forms for the other terms,

$$\begin{aligned}
|00\rangle \langle 10| &\mapsto i |10\rangle \langle 00|, & |00\rangle \langle 11| &\mapsto -i |10\rangle \langle 01|, & |10\rangle \langle 00| &\mapsto i |00\rangle \langle 10|, & |10\rangle \langle 01| &\mapsto -i |00\rangle \langle 11|, \\
|01\rangle \langle 10| &\mapsto -i |11\rangle \langle 00|, & |01\rangle \langle 11| &\mapsto i |11\rangle \langle 01|, & |11\rangle \langle 00| &\mapsto -i |01\rangle \langle 10|, & |11\rangle \langle 01| &\mapsto i |01\rangle \langle 11|. \tag{F11}
\end{aligned}$$

To understand how this procedure generalizes to bigger systems, it is easier to work with operators. It is important to note that the operator basis in the fermionic coherent state basis factorizes such that,

$$\begin{aligned}
|\{\xi_j\}\rangle \langle \{\bar{\chi}_j\}| &= \prod_j [e^{-\xi_j f_j^\dagger} (1 - f_j^\dagger f_j) e^{-f_j \bar{\chi}_j}] \\
&= \prod_j [1 - f_j^\dagger f_j - \xi_j f_j^\dagger + \bar{\chi}_j f_j + \xi_j \bar{\chi}_j f_j^\dagger f_j], \tag{F12}
\end{aligned}$$

and hence, the transformation (F6) reads

$$\begin{aligned}
U_T^{I_1} (|\{\xi_j\}_{j \in I_1}, \{\xi_j\}_{j \in I_2}\rangle \langle \{\bar{\chi}_j\}_{j \in I_1}, \{\bar{\chi}_j\}_{j \in I_2}|)^{T_1} [U_T^{I_1}]^\dagger \\
= \prod_{j \in I_1} [1 - f_j^\dagger f_j - i\xi_j f_j + i\bar{\chi}_j f_j^\dagger + \xi_j \bar{\chi}_j f_j^\dagger f_j] \cdot \prod_{j \in I_2} [1 - f_j^\dagger f_j - \xi_j f_j^\dagger + \bar{\chi}_j f_j + \xi_j \bar{\chi}_j f_j^\dagger f_j]. \tag{F13}
\end{aligned}$$

The above expression is equivalent to the simultaneous transformations

$$1 - f_j^\dagger f_j \mapsto 1 - f_j^\dagger f_j, \quad f_j^\dagger f_j \mapsto f_j^\dagger f_j, \quad f_j^\dagger \mapsto i f_j, \quad f_j \mapsto i f_j^\dagger, \quad \text{for } j \in I_1, \tag{F14}$$

which have the following form in the occupation number basis

$$|\{n_j\}_{j \in I_1}, \{\bar{n}_j\}_{j \in I_2}\rangle \langle \{\bar{n}_j\}_{j \in I_1}, \{\bar{n}_j\}_{j \in I_2}| \mapsto e^{i\phi(\{n_j\}, \{\bar{n}_j\})} |\{\bar{n}_j\}_{j \in I_1}, \{\bar{n}_j\}_{j \in I_2}\rangle \langle \{n_j\}_{j \in I_1}, \{\bar{n}_j\}_{j \in I_2}|, \quad n_j, \bar{n}_j \in \{0, 1\}, \tag{F15}$$

with the $U(1)$ phase $e^{i\phi(\{n_j\}, \{\bar{n}_j\})}$ determined by (F13). We should note that (F15) is the same as the bosonic partial transpose (F15) up to the presence of the $U(1)$ phase factor.

3. Partial transpose on fermionic operators

Here, we define the partial transpose on fermionic operators in the Fock space. Our goal is to determine how Majorana operators transform under the transformation rule defined by (F6) in the coherent state basis. This gives us an idea about what this transformation does compared to the known results in the literature for the partial transpose, e.g. Ref. [9]. Before we proceed, note that the transformation in (F6) consists of two steps: Taking the partial transpose $\rho_I^{T_1}$ and applying the unitary transformation $U_T^{I_1} \rho_I^{T_1} [U_T^{I_1}]^\dagger$. We will show what each step does to Majorana fermions.

Consider a system of N fermionic states. We introduce Majorana fermions

$$c_{2j-1} = f_j + f_j^\dagger, \quad c_{2j} = i(f_j - f_j^\dagger). \tag{F16}$$

Let

$$\rho_I = \sum_{\kappa, \tau, |\kappa| + |\tau| = \text{even}} w_{\kappa, \tau} c_{m_1}^{\kappa_1} \cdots c_{m_{2k}}^{\kappa_{2k}} c_{n_1}^{\tau_1} \cdots c_{n_{2l}}^{\tau_{2l}} \quad (\text{F17})$$

be the density matrix in the Majorana representation for the subsystem $I = I_1 \cup I_2 = \{m_1, \dots, m_{2k}\} \cup \{n_1, \dots, n_{2l}\}$. We use the notation $c_x^0 = \mathbb{I}$ and $c_x^1 = c_x$, so that $\kappa_i, \tau_j \in \{0, 1\}$. We also introduce the vectors (bit strings) $\kappa = (\kappa_1, \dots, \kappa_{2k})$, $\tau = (\tau_1, \dots, \tau_{2l})$, and their norms $|\kappa| = \sum_{j=1}^{2k} \kappa_j$, $|\tau| = \sum_{j=1}^{2l} \tau_j$. We assume the density matrix ρ_I commutes with the fermion parity operator $(-1)^{F_I} = \prod_{j=1}^k i c_{n_{2j-1}} c_{n_{2j}} \prod_{j=1}^l i c_{m_{2j-1}} c_{m_{2j}}$ on the subsystem I , which implies that the sum is over all possible bit strings provided that the constraint $|\kappa| + |\tau| = \text{even}$ is satisfied. Using this expression of the density matrix, we introduce the partial transpose for the subsystem I_1 in a similar fashion to Ref. [9],

$$\rho_I^{T_1} := \sum_{\kappa, \tau, |\kappa| + |\tau| = \text{even}} w_{\kappa, \tau} \mathcal{R}(c_{m_1}^{\kappa_1} \cdots c_{m_{2k}}^{\kappa_{2k}}) c_{n_1}^{\tau_1} \cdots c_{n_{2l}}^{\tau_{2l}}. \quad (\text{F18})$$

In the following, we show that the definition (F6) leads to the condition $\mathcal{R}(M_1 M_2) = \mathcal{R}(M_1) \mathcal{R}(M_2)$ for two operators M_1 and M_2 acting on the subsystem I_1 , which contrasts with Ref. [9] where \mathcal{R} is introduced to satisfy $\mathcal{R}(M_1 M_2) = \mathcal{R}(M_2) \mathcal{R}(M_1)$. Moreover, we see that Eq. (F6) dictates the choice $e^{i\theta} = \pm i$ for the $U(1)$ phase freedom in the partial transpose $\mathcal{R}(c) = e^{i\theta} c$ for a single Majorana fermion.

First, we need to introduce a TRS-dependent unitary operator $U_T^{I_1}$ on the subsystem I_1 . For the symmetry class BDI, TRS is defined in (F5) and the TRS operator is given by $\mathcal{T} = (\prod_j c_{2j-1}) \mathcal{K}$ where \mathcal{K} is the complex conjugation. Therefore, we define $U_T^{I_1}$ as a unitary part acting on the subsystem I_1 ,

$$U_T^{I_1} := \prod_{j \in I_1} c_{2j-1}. \quad (\text{F19})$$

Second, in order to determine the action of \mathcal{R} on Majorana operators, we compute both sides of (F6) separately and finally identify them. From the left-hand side of (F6), we get

$$\begin{aligned} & U_T^{I_1} (|\{\xi_j\}\rangle \langle \{\bar{\chi}_j\}|)^{T_1} [U_T^{I_1}]^\dagger \\ &= U_T^{I_1} \left[\prod_{j \in I_1} \left(\frac{1 + \xi_j \bar{\chi}_j}{2} - \frac{\xi_j - \bar{\chi}_j}{2} c_{2j-1} - i \frac{\xi_j + \bar{\chi}_j}{2} c_{2j} + \frac{i(1 - \xi_j \bar{\chi}_j)}{2} c_{2j-1} c_{2j} \right) \right]^{T_1} [U_T^{I_1}]^\dagger \\ &= \prod_{j \in I_1} c_{2j-1} \mathcal{R} \left[\prod_{n \in I_1} \left(\frac{1 + \xi_n \bar{\chi}_n}{2} - \frac{\xi_n - \bar{\chi}_n}{2} c_{2n-1} - i \frac{\xi_n + \bar{\chi}_n}{2} c_{2n} + \frac{i(1 - \xi_n \bar{\chi}_n)}{2} c_{2n-1} c_{2n} \right) \right] \prod_{j \in I_1}^{\leftarrow} c_{2j-1} \\ & \quad \cdot \prod_{n \in I_2} \left(\frac{1 + \xi_n \bar{\chi}_n}{2} - \frac{\xi_n - \bar{\chi}_n}{2} c_{2n-1} - i \frac{\xi_n + \bar{\chi}_n}{2} c_{2n} + \frac{i(1 - \xi_n \bar{\chi}_n)}{2} c_{2n-1} c_{2n} \right). \end{aligned} \quad (\text{F20})$$

where $[U_T^{I_1}]^\dagger = \prod_{j \in I_1}^{\leftarrow} c_{2j-1}$ which means that Majorana operators are arranged in the reversed order compared to that of $U_T^{I_1}$. The right-hand side of (F6) also yields

$$\begin{aligned} & |\{-i\bar{\chi}_j\}_{j \in I_1}, \{\xi_j\}_{j \in I_2}\rangle \langle \{-i\xi_j\}_{j \in I_1}, \{\bar{\chi}_j\}_{j \in I_2}| \\ &= \prod_{j \in I_1} \left(\frac{1 + \xi_j \bar{\chi}_j}{2} - \frac{i\xi_j - i\bar{\chi}_j}{2} c_{2j-1} - i \frac{-i\xi_j - i\bar{\chi}_j}{2} c_{2j} + \frac{i(1 - \xi_j \bar{\chi}_j)}{2} c_{2j-1} c_{2j} \right) \\ & \quad \cdot \prod_{j \in I_2} \left(\frac{1 + \xi_j \bar{\chi}_j}{2} - \frac{\xi_j - \bar{\chi}_j}{2} c_{2j-1} - i \frac{\xi_j + \bar{\chi}_j}{2} c_{2j} + \frac{i(1 - \xi_j \bar{\chi}_j)}{2} c_{2j-1} c_{2j} \right). \end{aligned} \quad (\text{F21})$$

Now, we compare the left-hand side (F20) and the right-hand side (F21) of Eq. (F6) by identifying the operators multiplying the same Grassmann variables. This identification in turn fixes the partial transpose $\mathcal{R}(c) = -ic$ and enforces the condition $\mathcal{R}(M_1 M_2) = \mathcal{R}(M_1) \mathcal{R}(M_2)$ (i.e., no reversed ordering). It is important to note that if we had reversed ordering, the right-hand side (F21) must have had terms like $\xi_{n-j} c_{2j-1}$ (i.e., we should have had reversed ordering of Grassmann variables in (F21) besides exchanging them from bra to ket states).

So far, we have shown that the cross-cap as defined by the path-integral can be recast as a change of Grassmann variables in the density matrix written in the coherent state basis. We have also found the equivalent transformation rules governed by $U_T^{I_1} \rho_I^{T_1} [U_T^{I_1}]^\dagger$ for the Majorana operators. In summary, the key equation of this section is

$$U_T^{I_1} \rho_I^{T_1} [U_T^{I_1}]^\dagger = \int d[\bar{\xi}] d[\xi] d[\bar{\chi}] d[\chi] e^{-\sum_j (\bar{\xi}_j \xi_j + \bar{\chi}_j \chi_j)} | \{-i\bar{\chi}_j\}_{j \in I_1}, \{\xi_j\}_{j \in I_2} \rangle \rho_I(\{\bar{\xi}_j\}; \{\chi_j\}) \langle \{-i\xi_j\}_{j \in I_1}, \{\bar{\chi}_j\}_{j \in I_2} |. \quad (\text{F22})$$

where $\rho_I(\{\bar{\xi}_j\}; \{\chi_j\}) = \langle \{\bar{\xi}_j\} | \rho_I | \{\chi_j\} \rangle$. The above expression is then used to numerically evaluate the topological invariant $Z_{\mathcal{T}} = \text{tr}(\rho_I U_T^{I_1} \rho_I^{T_1} [U_T^{I_1}]^\dagger)$ in the following sections.

4. Fermionic matrix product state

Here, we show how we compute the partial transpose for the fermionic MPS introduced in Eq. (D1). Consider a chain with N sites where I_1 corresponds to the sites $1, \dots, M_1$ and I_2 corresponds to the sites $M_1 + 1, \dots, M_1 + M_2 = M$. First, we need to compute the reduced density matrix, that is found to be

$$\begin{aligned} \rho_I &= \text{tr}_{S \setminus I} (|\Psi\rangle \langle \Psi|) \\ &= \int d[\xi] d[\bar{\xi}] e^{\sum_{xx'} \bar{\xi}^T(x) M_{xx'}^\dagger \bar{\xi}(x')} e^{\sum_{xx'} \xi^T(x) M_{xx'} \xi(x')} \\ &\quad \times e^{-\sum_{x \notin I} \bar{\xi}^T(x) \kappa \kappa^T \xi(x)} e^{\sum_{x \in I} \xi^T(x) \kappa f_x^\dagger} |0\rangle \langle 0| e^{\sum_{x \in I} f_x \kappa^T \bar{\xi}(x)}. \end{aligned} \quad (\text{F23})$$

where the matrix M is defined in Eq. (D13). Its partial transpose then becomes

$$\begin{aligned} U_T^{I_1} \rho_I^{T_1} [U_T^{I_1}]^\dagger &= \int d[\xi] d[\bar{\xi}] e^{\sum_{xx'} \bar{\xi}^T(x) M_{xx'}^\dagger \bar{\xi}(x')} e^{\sum_{xx'} \xi^T(x) M_{xx'} \xi(x')} \\ &\quad \times e^{-\sum_{x \notin I} \bar{\xi}^T(x) \kappa \kappa^T \xi(x)} e^{-\sum_{x \in I_1} i \bar{\xi}^T(x) \kappa f_x^\dagger + \sum_{x \in I_2} \xi^T(x) \kappa f_x^\dagger} |0\rangle \langle 0| e^{-\sum_{x \in I_1} i f_x \kappa^T \xi(x) + \sum_{x \in I_2} f_x \kappa^T \bar{\xi}(x)} \end{aligned} \quad (\text{F24})$$

Therefore, the overlap can be computed as follows

$$\begin{aligned} Z_{\mathcal{T}} &= \text{tr}(\rho_I U_T^{I_1} \rho_I^{T_1} [U_T^{I_1}]^\dagger) \\ &= \int d[\xi] d[\bar{\xi}] \int d[\eta] d[\bar{\eta}] e^{\sum_{xx'} \bar{\xi}^T(x) M_{xx'}^\dagger \bar{\xi}(x')} e^{\sum_{xx'} \xi^T(x) M_{xx'} \xi(x')} e^{\sum_{xx'} \bar{\eta}^T(x) M_{xx'}^\dagger \bar{\eta}(x')} e^{\sum_{xx'} \eta^T(x) M_{xx'} \eta(x')} \\ &\quad \times e^{-\sum_{x \notin I} \bar{\xi}^T(x) \kappa \kappa^T \xi(x)} e^{-\sum_{x \notin I} \bar{\eta}^T(x) \kappa \kappa^T \eta(x)} \\ &\quad \times e^{-\sum_{x \in I_1} i \bar{\xi}^T(x) \kappa \kappa^T \bar{\eta}(x) + \sum_{x \in I_2} \xi^T(x) \kappa \kappa^T \bar{\eta}(x)} e^{-\sum_{x \in I_1} i \eta(x) \kappa \kappa^T \xi(x) + \sum_{x \in I_2} \eta(x) \kappa \kappa^T \bar{\xi}(x)} \\ &= \int d[\xi] d[\bar{\xi}] \int d[\eta] d[\bar{\eta}] \exp \left[(\xi^T, \bar{\xi}^T, \eta^T, \bar{\eta}^T) \tilde{W} (\xi^T, \bar{\xi}^T, \eta^T, \bar{\eta}^T)^T \right] \\ &= \text{Pf}[\tilde{W}]. \end{aligned} \quad (\text{F25})$$

The matrix \tilde{W} is given by

$$\tilde{W} = \begin{pmatrix} \tilde{Y} & -V \\ V^T & \tilde{Y} \end{pmatrix}, \quad (\text{F27})$$

where \tilde{Y} and V are a $2N \times 2N$ matrix defined by

$$\tilde{Y} = \begin{pmatrix} M & -K_1 \\ K_1^T & M^\dagger \end{pmatrix}, \quad (\text{F28})$$

and

$$V = \begin{pmatrix} K_2 & K_3 \\ K_3 & K_2 \end{pmatrix}. \quad (\text{F29})$$

5. Grassmann representation of BdG ground state

In Appendix B, we show that the ground state of the BdG Hamiltonian can be written in the form of Eq. (B8) in terms of the matrix ϕ_{ij} . Inspired by the results of fermionic MPS in the previous appendix, we can reverse engineer the process and introduce the wave function

$$|\Psi\rangle = \int d[\xi] e^{\sum_{ij} \xi_i [\phi^{-1}]_{ij} \xi_j} e^{\sum_j \xi_j f_j^\dagger} |0\rangle. \quad (\text{F33})$$

It is straightforward to see that the above wave function is identical to the BdG wave function (Eq. (B8)) as one carries out the Gaussian integral over ξ_j variables. Alternatively, we can start by representing the wave function in the coherent state basis

$$\begin{aligned} |\Psi\rangle &= \int d[\xi] d[\bar{\xi}] e^{-\sum_j \bar{\xi}_j \xi_j} \langle \xi | \Psi \rangle | \xi \rangle \\ &= \int d[\xi] d[\bar{\xi}] e^{-\sum_j \bar{\xi}_j \xi_j} \langle \bar{\xi} | e^{\sum_{ij} f_i^\dagger \phi_{ij} f_j^\dagger} | 0 \rangle | \xi \rangle \\ &= \int d[\xi] d[\bar{\xi}] e^{-\sum_j \bar{\xi}_j \xi_j} e^{\sum_{ij} \bar{\xi}_i \phi_{ij} \bar{\xi}_j} | \xi \rangle, \end{aligned} \quad (\text{F34})$$

and carry out the Gaussian integral over $\bar{\xi}$ variables to arrive at (F33). Therefore, we can use the procedure explained in the previous appendix to compute the partial transpose $Z_{\mathcal{T}}$ with no difficulty. The result is shown in Fig. 4 of the main text. The important point here is that by using the Grassmann representation, the action of time-reversal operator becomes a change of variables in the space of Grassmann variables.

6. Fixed-point wave function

Here, we explicitly compute $Z_{\mathcal{T}}$ for the ground state wave function of the fixed-point Hamiltonian of Majorana chain introduced in Eq. (C3). Let $I_1 = \{1, 2, \dots, M_1\}$, $I_2 = \{M_1 + 1, \dots, M\}$ be adjacent intervals on closed circle S . First, we cut the system along the boundary of I . As a result, we are left with 6 Majorana zero modes

$$c_0^R \quad c_1^L \quad c_{M_1}^R \quad c_{M_1+1}^L \quad c_M^R \quad c_{M+1}^L \quad (\text{F35})$$

The Hilbert space of I_1 , I_2 , and $S \setminus I$ consist of the fermions

$$f_1^\dagger = \frac{c_1^L - ic_{M_1}^R}{2}, \quad f_2^\dagger = \frac{c_{M_1+1}^L - ic_M^R}{2}, \quad f_3^\dagger = \frac{c_{M+1}^L - ic_0^R}{2}, \quad (\text{F36})$$

respectively. The corresponding terms in the Hamiltonian (Eq. (C3)) are

$$H_I = i(c_0^R c_1^L + c_{M_1}^R c_{M_1+1}^L + c_M^R c_{M+1}^L). \quad (\text{F37})$$

The ground state of this Hamiltonian is given by

$$|\Psi\rangle = \frac{1}{2} [(1 + f_1^\dagger f_2^\dagger) f_3^\dagger |0\rangle + (f_1^\dagger + f_2^\dagger) |0\rangle]. \quad (\text{F38})$$

The total density matrix for the ground state is

$$\rho = |\Psi\rangle \langle \Psi| = \frac{1}{4} \left[(1 + f_1^\dagger f_2^\dagger) |0\rangle \langle 0| (1 + f_2 f_1) + (f_1^\dagger + f_2^\dagger) f_3^\dagger |0\rangle \langle 0| f_3 (f_1 + f_2) + \dots \right], \quad (\text{F39})$$

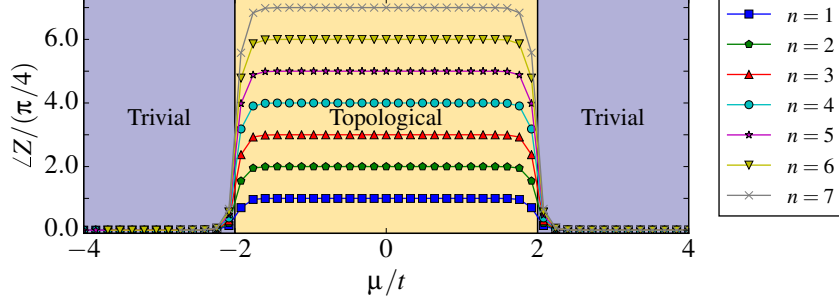


FIG. 6. Additivity of the complex phase for $Z_{\mathcal{T}}$ computed on a single Majorana chain with n intervals. Here, $t = \Delta$, total system size is $N = 2nN_{\text{part}}$, and $N_{\text{part}} = 20$.

where ellipses refer to the off-diagonal terms. This gives rise to the reduced density matrix

$$\begin{aligned} \rho_I = \text{tr}_3 \rho &= \frac{1}{4} \left[(1 + f_1^\dagger f_2^\dagger) |0\rangle \langle 0| (1 + f_2 f_1) + (f_1^\dagger + f_2^\dagger) |0\rangle \langle 0| (f_1 + f_2) \right] \\ &= \frac{1}{4} \begin{pmatrix} 1 & 0 & 0 & 1 \\ 0 & 1 & 1 & 0 \\ 0 & 1 & 1 & 0 \\ 1 & 0 & 0 & 1 \end{pmatrix} = \frac{1}{4} (1 + \sigma_1 \otimes \sigma_1), \end{aligned} \quad (\text{F40})$$

where the density matrix is represented in the basis $\{|0\rangle, f_1^\dagger |0\rangle, f_2^\dagger |0\rangle, f_1^\dagger f_2^\dagger |0\rangle\}$ and σ_i is Pauli matrices. This can also be written in terms of Majorana operators

$$\begin{aligned} \rho_I &= \frac{1}{4} (1 + f_1^\dagger f_2^\dagger + f_2 f_1 + f_2^\dagger f_1 + f_1^\dagger f_2) \\ &= \frac{1}{4} (1 - i c_{M_1}^R c_{M_1+1}^L). \end{aligned} \quad (\text{F41})$$

The partial transpose is given by

$$U_T^{I_1} \rho_I^{T_1} [U_T^{I_1}]^\dagger = \frac{1}{4} (1 + c_{M_1}^R c_{M_1+1}^L) = \frac{1}{4} (1 + i \sigma_1 \otimes \sigma_1), \quad (\text{F42})$$

where $U_T^{I_1} = c_1^L$. The SPT invariant is found by

$$\begin{aligned} Z_{\mathcal{T}} &= \text{tr} (\rho_I U_T^{I_1} \rho_I^{T_1} [U_T^{I_1}]^\dagger) \\ &= \text{tr} \left[\frac{1}{4} (1 + \sigma_1 \otimes \sigma_1) \frac{1}{4} (1 + i \sigma_1 \otimes \sigma_1) \right] \\ &= \frac{1+i}{4} = \frac{1}{2\sqrt{2}} e^{i\pi/4}. \end{aligned} \quad (\text{F43})$$

Similarly for $e^{i\theta} = -i$, we get $Z_{\mathcal{T}} = \frac{1}{2\sqrt{2}} e^{-i\pi/4}$. Thus, we reproduce the \mathbb{Z}_8 classification for the symmetry class BDI.

Let us now check that the \mathbb{Z}_8 topological phase derived from the partial transpose of the Majorana chain is additive under including additional fermion flavors or twist defects. In other words, if we include n fermion flavors or introduce n twist defects, the resulting complex phase computed by the partial transpose or the partial reflection will be $e^{in\pi/4}$. Let us first show this result analytically for the fixed-point wave function. Using Eq. (F41), the reduced density

matrix for n flavors of fermions is given by

$$\begin{aligned}\rho_I &= \bigotimes_{\alpha=1}^n \rho_{I,\alpha} \\ &= \frac{1}{4^n} \prod_{\alpha=1}^n (1 - i c_{1,\alpha}^R c_{2,\alpha}^L).\end{aligned}\quad (\text{F44})$$

where c_1 and c_2 refer to the Majorana zero modes located at the ends of each interval and the index $\alpha = 1, \dots, n$ is associated with fermion flavors corresponding to n chains or n intervals on a single chain. To obtain the partial transpose, we must first compute $\rho_I^{T_1}$,

$$\begin{aligned}\rho_I^{T_1} &= \frac{1}{4^n} \prod_{\alpha=1}^n (1 - i \mathcal{R}(c_{1,\alpha}^R) c_{2,\alpha}^L) \\ &= \frac{1}{4^n} \prod_{\alpha=1}^n (1 + c_{1,\alpha}^R c_{2,\alpha}^L).\end{aligned}\quad (\text{F45})$$

Therefore, the partial transpose $Z_{\mathcal{T}}$ is found by

$$\begin{aligned}Z_{\mathcal{T}} &= \text{tr}(\rho_I U_T^{I_1} \rho_I^{T_1} [U_T^{I_1}]^\dagger) \\ &= \frac{1}{4^n} \text{tr} \left[\prod_{\alpha=1}^n (1 - i c_{1,\alpha}^R c_{2,\alpha}^L) \prod_{\beta=1}^n c_{1,\beta}^L \prod_{\alpha'=1}^n (1 + c_{1,\alpha'}^R c_{2,\alpha'}^L) \prod_{\beta'=1}^n c_{1,\beta'}^L \right] \\ &= \frac{1}{4^n} \text{tr} \left[\prod_{\alpha=1}^n (1 + i) + \dots \right] \\ &= \frac{1}{(2\sqrt{2})^n} e^{in\pi/4},\end{aligned}\quad (\text{F46})$$

where ellipses represent the off-diagonal terms.

For further verification of additivity, we numerically compute the partial transpose for n separated intervals on a single chain. As we see in Fig. 6 the resulting complex phase in the topological regime is $e^{in\pi/4}$, as expected.

Appendix G: Three-dimensional inversion symmetric topological superconductor (Class D + inversion)

As we have seen in the main text, the symmetry class D with inversion symmetry in three dimension is classified by \mathbb{Z}_{16} . To compute the partial inversion, we use the generating model in this symmetry class, which is given by the BdG Hamiltonian

$$\hat{H} = \frac{1}{2} \sum_{\mathbf{k}} \Psi^\dagger(\mathbf{k}) h(\mathbf{k}) \Psi(\mathbf{k}), \quad (\text{G1})$$

on a cubic lattice, where

$$\Psi^\dagger(\mathbf{k}) = (f_\uparrow^\dagger(\mathbf{k}), f_\downarrow^\dagger(\mathbf{k}), f_\downarrow(-\mathbf{k}), -f_\uparrow(-\mathbf{k})), \quad (\text{G2})$$

and

$$h(\mathbf{k}) = [-t(\cos k_x + \cos k_y + \cos k_z) - \mu] \tau_z + \Delta [\sin k_x \tau_x \sigma_x + \sin k_y \tau_x \sigma_y + \sin k_z \tau_x \sigma_z]. \quad (\text{G3})$$

in which the τ and σ matrices act on particle-hole and spin subspaces, respectively. This Hamiltonian also describes the $^3\text{He-B}$ phase. The inversion symmetry in this model is defined by

$$\mathcal{I} f_\sigma(x, y, z) \mathcal{I}^{-1} = i f_\sigma(-x, -y, -z). \quad (\text{G4})$$

We set $t = \Delta = 1$. This model exhibits three different topological phases as follows:

1. $1 < |\mu| < 3$: Topological I. This phase hosts a 2d gapless Majorana surface states. The corresponding interacting classification is \mathbb{Z}_{16} .
2. $|\mu| < 1$: Topological II. This phase supports an even number of 2d gapless Majorana surface states. It is topologically equivalent to a stack of 2d topological superconductors in the same symmetry class. Therefore, the corresponding classification is \mathbb{Z}_8 .
3. $|\mu| > 3$: Trivial. No topological surface states.

We use the above definition of the inversion operator and transform a subset (cubic subsystem) of the lattice sites to compute the overlap function using Eq. (B12). The results are shown in Fig. 5 of the main text and completely match with those expected from the bordism theory.

Appendix H: Effect of disorder on partial reflection

In this appendix, we check the robustness of the partial reflection and compute the \mathbb{Z}_8 invariant for class D (with reflection symmetry) in the presence of a chemical potential disorder. We also map out the phase diagram of the disordered Majorana chain and reproduce the known results [12, 13]. The Hamiltonian is given by $H = H_{\text{clean}} + H_{\text{dis}}$ where H_{clean} is the Hamiltonian of the Majorana chain (Eq. (1) of main text), the disorder term is

$$H_{\text{dis}} = \sum_x v_x f_x^\dagger f_x, \quad (\text{H1})$$

and v_x is a random number uniformly distributed over the range $[-W/2, W/2]$ where W is the disorder strength. Figure 7 shows the complex phase of the averaged partial reflection for various values of W over a wide range of chemical potential including the trivial and topological phases. It is interesting to note that the topological region (characterized by $\angle Z = \pi/4$) expands a little bit as the disorder strength is increased. This is similar to the disorder induced topological phase due to quadratic corrections on the lattice models which has been discussed in the context of the 2D and 3D topological insulators [14–16]. In addition, we provide the complex phase of the partial reflection for one realization of disorder in Fig. 8. It is evident from this figure that the phase is quite robust to a moderate disorder.

We use the complex phase associated with the partial reflection to map out the phase diagram of the disordered Majorana chain as shown in Fig. 9(b). For reference, we compute the phase boundary between the trivial and topological phases as a function of disorder strength W , using the transfer matrix approach [12, 13] (see Fig. 9(a)). In the case of our model, the Majorana chain with nearest neighbor hopping, the Lyapunov exponent can be found analytically,

$$\begin{aligned} \Lambda^{-1} &= \left| \lim_{n \rightarrow \infty} \frac{1}{n} \sum_{j=1}^n \ln \left| \frac{\mu + v_j}{2t} \right| \right| \\ &= \left| \int_{-1/2}^{1/2} dx \ln \left| \frac{\mu + xW}{2t} \right| \right| \\ &= \left| \ln \left[\frac{|2\mu + W| \frac{\mu}{W} + \frac{1}{2}}{|2\mu - W| \frac{\mu}{W} - \frac{1}{2}} \right] - (1 + \ln 2t) \right| \end{aligned} \quad (\text{H2})$$

and the phase boundary is given by a line of critical points in which $\Lambda \rightarrow \infty$ is diverging. The diverging Λ is indicative of delocalized states at zero chemical potential which are in turn responsible for the topological phase transition. We show in Fig. 9(b) that the transfer matrix and our results are in remarkable agreement.

Appendix I: Partial reflection for projected wave functions

In this appendix, we present the results for the projected wave functions, i.e., we look at the wave function with a fixed number of particles and show that the \mathbb{Z}_8 classification survives in this case, too. The wave function is obtained by projecting the BCS wave function as in

$$|\Psi_{\bar{n}}\rangle = \mathcal{P}_{\bar{n}} |\Psi_{\text{BCS}}\rangle \quad (\text{I1})$$

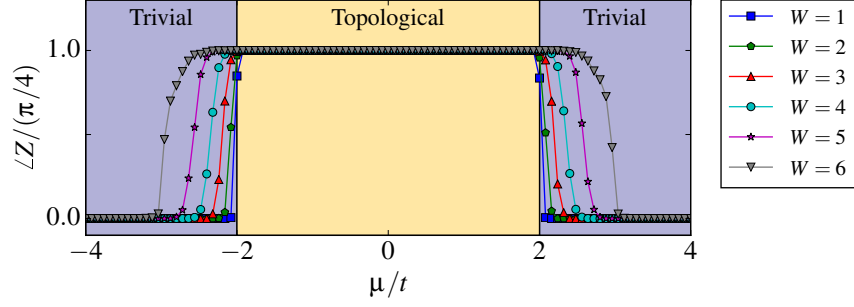


FIG. 7. Complex phase of the partial reflection for the disordered Majorana chain. Each curve represents an ensemble average over 1000 samples. Solid lines are guides for the eye. Here, we set $\Delta = t$, $N = 200$ and $N_{\text{part}} = 100$.

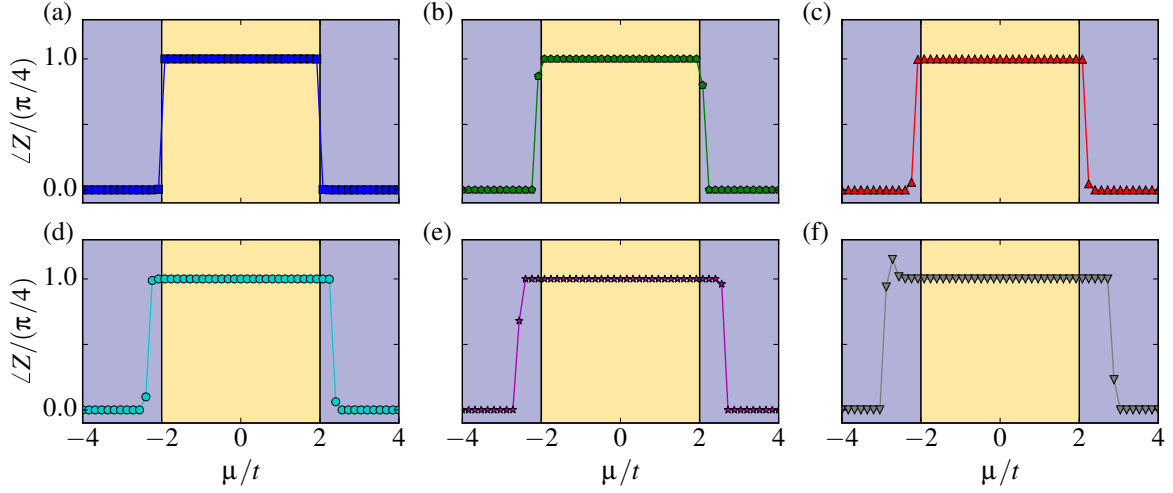


FIG. 8. Complex phase of the partial reflection for one realization of the disorder potential. Panels (a)-(f) represent different disorder strength from $W = 1$ to $W = 6$ (same as the legend in Fig. 7). Solid lines are guides for the eye. Here, we set $\Delta = t$, $N = 200$ and $N_{\text{part}} = 100$.

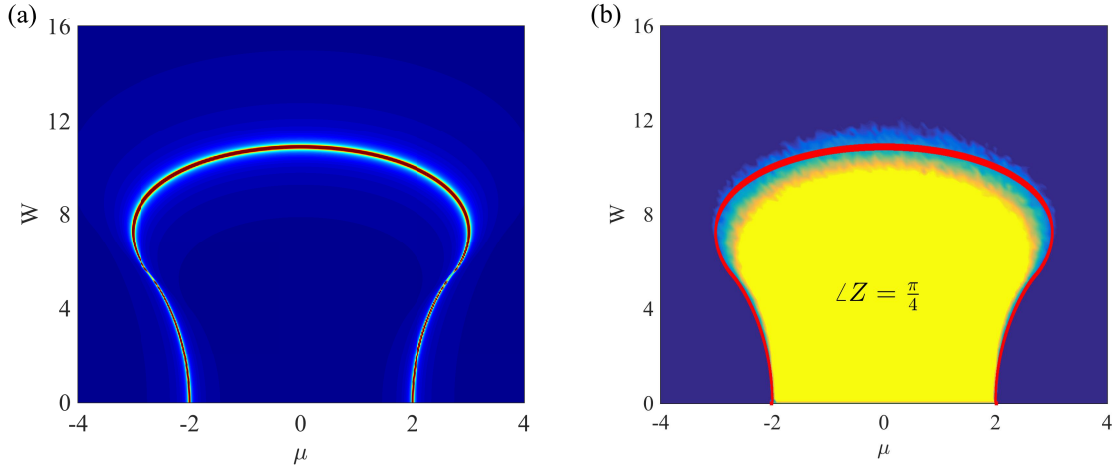


FIG. 9. Phase diagram of the disordered Majorana chain, using (a) transfer matrix (which is computed analytically, Eq. (H2)), (b) partial reflection. In panel (b), the red curve shows the phase boundary which is analytically determined by the transfer matrix as shown in (a). Here, we set $\Delta = t$, $N = 200$ and $N_{\text{part}} = 100$.

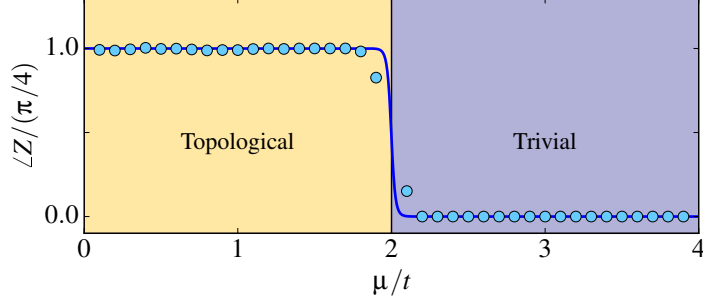


FIG. 10. Complex phase of the partial reflection for the projected BCS wave function (Eq. (I1)). Solid line shows the result for the mean-field BCS wave function (Fig. 3 in the main text). Here, we set $\Delta = t$, $N = 200$ and $N_{\text{part}} = 100$.

where $\mathcal{P}_{\bar{n}}$ is the projection operator to the averaged particle number of the BCS wave function, i.e.,

$$\bar{n} = \langle \Psi_{\text{BCS}} | \sum_x f_x^\dagger f_x | \Psi_{\text{BCS}} \rangle = \sum_k |v_k|^2 \quad (\text{I2})$$

and

$$|\Psi_{\text{BCS}}\rangle = \prod_{k>0} (u_k + v_k f_k^\dagger f_{-k}^\dagger) |0\rangle. \quad (\text{I3})$$

$|\Psi_{\bar{n}}\rangle$ is usually used as a good trial wave function with a fixed number of particles corresponding to the $|\Psi_{\text{BCS}}\rangle$. We construct the BCS wave function from the Majorana chain Hamiltonian (Eq. (2) of main text), where the coefficients are given by

$$u_k^2 = \frac{1}{2} \left(1 + \frac{\varepsilon_k - \mu}{\sqrt{(\varepsilon_k - \mu)^2 + \Delta_k^2}} \right), \quad (\text{I4})$$

$$v_k^2 = \frac{1}{2} \left(1 - \frac{\varepsilon_k - \mu}{\sqrt{(\varepsilon_k - \mu)^2 + \Delta_k^2}} \right), \quad (\text{I5})$$

in which $\varepsilon_k = -2t \cos k$ and $\Delta_k = 2\Delta \sin k$. To evaluate the partial reflection for the projected wave functions, we define a real-space representation of the wave function as introduced in Eq. (B15). Next, we use variational Monte Carlo to compute the wave function overlap

$$Z = \langle \Psi_{\bar{n}} | \tilde{\Psi}_{\bar{n}} \rangle = \frac{\sum_c \langle \Psi_{\bar{n}} | c \rangle \langle c | \tilde{\Psi}_{\bar{n}} \rangle}{\left[\sum_c |\langle c | \Psi_{\bar{n}} \rangle|^2 \sum_{c'} |\langle c' | \tilde{\Psi}_{\bar{n}} \rangle|^2 \right]^{1/2}} \quad (\text{I6})$$

where

$$|\tilde{\Psi}_{\bar{n}}\rangle = \mathcal{R}_{\text{part}} \mathcal{P}_{\bar{n}} |\Psi\rangle \quad (\text{I7})$$

is the reflected wave function after the projection and the configuration $c = \{r_1, r_2, \dots, r_{\bar{n}}\}$ refers to the positions of the \bar{n} particles. The results are shown in Fig. 10 which are in excellent agreement with the mean-field BCS wave functions.

-
- [1] C.-K. Chiu, H. Yao, and S. Ryu, *Phys. Rev. B* **88**, 075142 (2013).
 - [2] T. Morimoto and A. Furusaki, *Phys. Rev. B* **88**, 125129 (2013).
 - [3] K. Shiozaki and M. Sato, *Phys. Rev. B* **90**, 165114 (2014).
 - [4] J. Dubail and N. Read, *Phys. Rev. B* **92**, 205307 (2015).
 - [5] H. Katsura, D. Schuricht, and M. Takahashi, *Phys. Rev. B* **92**, 115137 (2015).

- [6] M. Greiter, V. Schnells, and R. Thomale, [arXiv: 1402.5262](#) (2014).
- [7] R. M. Lutchyn, J. D. Sau, and S. Das Sarma, *Phys. Rev. Lett.* **105**, 077001 (2010).
- [8] A. Kapustin, R. Thorngren, A. Turzillo, and Z. Wang, *Journal of High Energy Physics* **2015**, 1 (2015).
- [9] V. Eisler and Z. Zimborás, *New Journal of Physics* **17**, 053048 (2015).
- [10] K. Shiozaki and S. Ryu, [arXiv: 1607.06504](#) (2016).
- [11] P. Calabrese, J. Cardy, and E. Tonni, *Journal of Statistical Mechanics: Theory and Experiment* **2013**, P02008 (2013).
- [12] I. Mondragon-Shem, T. L. Hughes, J. Song, and E. Prodan, *Phys. Rev. Lett.* **113**, 046802 (2014).
- [13] J. Song and E. Prodan, *Phys. Rev. B* **89**, 224203 (2014).
- [14] C. W. Groth, M. Wimmer, A. R. Akhmerov, J. Tworzydło, and C. W. J. Beenakker, *Phys. Rev. Lett.* **103**, 196805 (2009).
- [15] S. Ryu and K. Nomura, *Phys. Rev. B* **85**, 155138 (2012).
- [16] K. Kobayashi, T. Ohtsuki, and K.-I. Imura, *Phys. Rev. Lett.* **110**, 236803 (2013).